Interactive comment on "Multi-proxy reconstructions of May–September precipitation field in China over the past 500 years"

Feng Shi[1,2*], Sen Zhao[3,4], Zhengtang Guo[1,5,6], Hugues Goosse[2], Qiuzhen Yin[2]

[1]Key Laboratory of Cenozoic Geology and Environment, Institute of Geology and Geophysics, Chinese Academy of Sciences, Beijing, 100029, China

[2]Georges Lemaître Centre for Earth and Climate Research, Earth and Life Institute, Université catholique de Louvain, Louvain-la-Neuve, 1348, Belgium

[3]Key Laboratory of Meteorological Disaster of Ministry of Education, and College of Atmospheric Science, Nanjing University of Information Science and Technology, Nanjing, 210044, China

[4]School of Ocean and Earth Sciences and Technology, University of Hawaii at Mānoa, Honolulu, HI, 96822, USA

[5]CAS Center for Excellence in Tibetan Plateau Earth Sciences, Beijing, 100101, China

[6]University of Chinese Academy of Sciences, Beijing, 100049, China

Correspondence to: Feng SHI (shifeng@mail.iggcas.ac.cn)

- In blue: referees' comments

- In black: our answers

- In black italic: what we have added in the text

I. Response to reviewer 1:

General comments:

The manuscript presents a reconstruction of the seasonal mean precipitation in China over the past few centuries based on a collection of proxy records, comprising mostly tree-ring width and historical documents, but also included some oxygen isotopes record and a long Korean precipitation instrumental record. The statistical method to reconstruct the spatially resolved precipitation is a variant of Point-by-point regression, a method that has been applied for the generation of the Drought Atlases in other continental regions of the world by E. Cook and collaborators. I assume that other reviewers will comment on the quality and adequacy of the proxy records. Here I will mostly focus on the other aspects of the manuscript, like the statistical method applied,

the interpretation of the results - connection of the reconstructed precipitation to largescale variability modes, and on the clarity of the manuscript itself.

In general terms, I think this is a valuable study. The main conclusions related to the past spatial structure of the precipitation variability, indicating the presence of spatial dipoles at decadal timescales, and the lack of a clear connection to the external forcing are interesting, although maybe to some extend to be expected, and some were already hinted at in previous studies. However, I think the manuscript itself requires some technical revisions, not dramatic, but indeed careful. The language is sometimes not specific enough and could be misinterpreted by some readers. Also, the structure of one section - the discussion-is strange. This section actually contains further results and not so much a discussion about the results. All in all, I would recommend the publication after some revisions, as specified below. Some of my points are related to language usage, but those are more recommendations to check, as I am not a native English speaker

Response: We would like to thank the reviewer for his/her constructive review, comments, and suggestions, which have helped us to greatly improve our manuscript. We have done our best to address the reviewer's concerns and modified the manuscript in light of the reviewer's suggestions. In particular, we have modified the structure and the discussion following the reviewer's advice. Point-by-point responses to the comments are listed below.

Major comments:

Item 1: 1. The title could be more specific. The study reconstructs seasonal mean precipitation, so it should indicate the season

Response: The title has been revised to "*Multi-proxy reconstructions of May–September precipitation field in China over the past 500 years*" according to the reviewer's suggestion.

Item 2: 2. relationships with instrumental climate data (Fritts, 1976; Zhang, 1991). Other proxy records (e.g., ice core, coral, and varve sediment) have been introduced into regional climate field reconstructions (e.g., Neukom et al., 2011), but they are generally harder to use.

This is an example of what I meant by unspecific language, which can be also seen in other parts of the manuscript. What does 'harder to use' mean? I guess the difficulties are related to dating and time resolution, but the authors could be more specific and do not leave the reader guessing.

Response: The sentence has been revised to "*they generally represent a small percentage of the data available in global compilations (e.g. PAGES-2k-Consortium, 2013).*", according to the reviewer's suggestion. Moreover, the other parts of the manuscript have also checked and polished.

Item 3: 3. The targets for reconstructions are primarily on temperature variables or

variables related to temperature b

The targets are temperature or temperature-related variables.

Response: The sentence has been revised to "*The reconstruction targets are first temperature or temperature-related variables.*", according to the reviewer's suggestion.

Item 4: 4. large spatial coherency. Reconstructions of the localized precipitation field or other variables related to precipitation are seldom (Cook et al., 2004; Cook et al., 2015b; Seftigen et al., 2015) because they require proxy records with more extensive distributions. In particular, the Palmer Drought Severity Index (PDSI) Atlases over the past millennium in North America

I think the authors do not mean more extensive spatial distribution, but rather a more dense proxy network that it would be the case for temperature.

Response: The sentence has been revised to "… *because they require more dense proxy network that it would be the case for temperature*", according to the reviewer's suggestion.

Item 5: 5. The climate field reconstruction method can be divided into the Empirical Orthogonal Function-based (EOF-based) method (Mann et al., 2009) and the point-to-point regression-based (PPR-based) method (Cook et al., 1999). The core function of the

I had real problems with this sentence. I think I understand what the authors mean, but the sentence can be really misleading. First, there are more 'families' of reconstruction methods - consider for instance the Bayesian Hierarchical Modelling Barcast, or the methods based on Canonical Correlation, or the more modern methods based on offline data assimilation (e.g. Steiger and Hakim) or even the method based on particle filters. Also, the RegEM method used by Mann et al is not really 'EOF-based. It is correct that Mann et al used an EOF pre-filtering within the RegEM method, but this is not required by the algorithm itself. Therefore, I do not think that this sentence is really correct. The authors may want to re-consider according with what I think they really want to say. They probably mean that statistical methods may include an EOF-prefiltering of the predictand or of the predictor or of both, or not pre-filtering at all. In the former case some small-scale information is lost - I think this is what the authors are pointing to.

Response: Following the reviewer's suggestion, we have rewritten the review of the reconstruction methods as proposed below:

The paleoclimate reconstruction methods are divided into climate index reconstruction (CIR) method and climate field reconstruction (CFR) method according to the reconstruction target. The CIRs are mainly derived from two classes of method, direct regression and indirect regression (Christiansen and Ljungqvist, 2017). Methods using the climate variables as the predictands (or dependent variable) and the proxies as the predictors (or independent variable) are called direct regression. On the contrary, the climate variables as the predictors and the proxies as the predictands leads to

indirect regression. The composite plus scale (CPS) method is a widely used, classic direct regression, which composites a group of proxy records using uniform or proxy-dependent weighting. The time series obtained is then scaled to have the same variance as the targeted regional or hemispheric averaged variable over a chosen interval. More generally, the regression process is usually based on some forms of univariate or multivariate linear regression and the regression parameters are estimated using classic methods e.g. ordinary least squares, total least squares, variance matching. However, the problem is generally ill-posed because of the limited number of samples in the calibration period and regularized methods have to be introduced, e.g. truncated principal component regression (truncated-PCR) (Mann et al., 1999), Regularized Expectation Maximization (RegEM) (Mann et al., 2008), and Least Absolute Shrinkage and Selection Operator (LASSO) (McShane and Wyner, 2011).

The local (LOC) method is a promising method based on indirect regression. In the LOC method, each proxy record should be first calibrated using the local instrumental climate data, and the time series are then averaged to obtain the large-scale mean climate index (Christiansen, 2011). An indirect regression is used for the local calibration, justified by the fact that the proxy records are functions of climate variables and not the opposite. The reconstructions based on the LOC method are assumed to better preserve the low-frequency climate signal compared to other methods, though they would overestimate the high-frequency signal (Christiansen and Ljungqvist, 2011). Then, the optimal information extraction (OIE) method was proposed to address this bias using the arithmetic mean of the regression coefficients of the linear regression and the inverse regression (Shi et al., 2012). The hypothesis in the OIE method is that the regression coefficients are random variables with normal distribution that vary in the ranges between the classic linear regression and inverse regression. Additional methods have also been proposed recently to take into account some of the biases of classical methods based on regression such as the pairwise comparison (Hanhijärvi et al., 2013) or Bayesian method of various levels of complexity (e.g., Tingley and Huybers, 2010)).

The CFR methods can be divided into the reduced space objective analysis-based method (Evans et al., 2000) and the point-to-point regression-based (PPR-based) method (Cook et al., 1999). A typical example of the first group of method is provided by the study of Mann et al. (2009) in which the time coefficients of dominant EOF patterns, calculated from instrumental climate data, are estimated over the pre-instrumental data using a network of proxy records, and then, the climate field over the pre-instrumental data is attained from the product of the reconstructed time coefficients and the instrumental dominant EOF patterns. The underlying hypothesis is that the primary spatial modes of climate change during the instrumental period also explain a large fraction of the variability in the past. The advantage of this assumption is that only a few proxy records with sparse spatial coverage can be enough to reconstruct a climate field (Neukom et al., 2011). However, the discarded EOF patterns after EOF-truncation may retain some small-scale spatial information, which would have been lost. For instance, the global temperature field reconstruction (Mann et al., 2009) was

not consistent with a regional temperature field reconstruction in western Qinling Mountains, China (Yang et al., 2013b). In addition, this method is not well adapted for reconstructions of precipitation field because of the high spatial heterogeneity of this variable (Gómez-Navarro et al., 2015).

The PPR-based method reconstructs each grid point using a linear regression; e.g., PCR (Cook et al., 1999), RegEM regression (Shi et al., 2015a) or the OIE method (Yang et al., 2016) through searching candidate proxy records near the target. The goal of the PPR-based method is to maximizes the retention of spatial information, but this method requires a sufficient number of suitable proxy records near the objective grid points. Selecting only one type of proxy records, with the associated limited spatial distribution, hinders the field reconstruction of precipitation (or of a variable sensitive to precipitation) for a large-scale region using the PPR-based method. For example, the tree-ring based reconstruction of the MADA provides significant insights into past drought patterns in eastern Asia (Cook et al., 2010), but it performs poorly in reproducing dryness and wetness in eastern China because it only incorporates data from one short tree-ring width chronology from eastern China. Consequently, it would be invalid to extrapolate objective gridded drought variability on the basis of remote tree-ring records in western China (Yang et al., 2013a). Thus, one method to fully consider regional patterns of precipitation is to use the PPR-based method in conjunction with multi-proxy records with good spatial coverage.

Item 6: 6. The left EOF patterns may retain some useful regional spatial information, which would have been partially lost in the EOF- based method. For instance, the global temperature field reconstruction using the EOF-based method (Mann et al., 2009) was

The 'left patterns' is unfortunate. It may be misinterpreted as 'left and right vectors' in SVD. I would rather used 'the discarded EOF patterns after EOF-truncation

Response: According to the reviewer's suggestion, these words have been changed with "*the discarded EOF patterns after EOF-truncation…*".

Item 7: 7. (Shi et al., 2015a) and the optimal information extraction (OIE) method (Yang et al., 2016). In theory, the PPR-based method maximizes the retention of spatial information, but this method requires a sufficient number of suitable proxy

I also had problems with the description of the OIE method, and also to figure out to what extent this method is different from the PPR method. This manuscript does not give enough details and refers to other previous manuscript by Shi et al. I have quickly looked into those papers and I cannot tell the difference between OIE and PPR. This may be my probable, or the problem in previous manuscripts, but I really would recommend to be much more specific here, and at least indicate the basic difference between OIE and PPR, and what are the advantages, if any, of OIE over PPR in this setting.

Response: Following the reviewer's suggestion, we have rewritten the review of these reconstruction methods to explain the difference between OIE and PPR. In our

interpretation, the foundation of the PPR method is that the climate field reconstruction should be obtained through a reconstruction for each grid point. The OIE method belongs to an indirect regression method group, which can be used to reconstruct a climate index or a climate field. The OIE method is based, as for the LOC method, on the principle that the reconstruction process should be based on the fact that the proxy records are functions of climate variables. The main differences between OIE method and other methods are that the correlation coefficients between the local instrumental climate data and the target climate data are used in the computation of the weights in the regression, and the regression coefficients are random variables with normal distribution and vary in the ranges between the classic linear regression and inverse regression to obtain an uncertainty estimation.

Item 8: 8 The precipitation (or the variable sensitive to precipitation) field reconstruction for a large-scale region using the PPR-based method is difficult when only one type of proxy records did not cover all reconstruction areas. For example, the tree-ring

This sentence is too cumbersome. I think I understand what it means, but the authors may consider rephrasing.

Response: The sentence has been revised to "*Selecting only one type of proxy records, with the associated limited spatial distribution, hinders the field reconstruction of precipitation (or of a variable sensitive to precipitation) for a large-scale region using the PPR-based method.*", according to the reviewer's suggestion.

Item 9: 9. regression and inverse regression. The LOC regression method has already been verified to efficiently retain low-frequency climate signals (Christiansen, 2011; Shi et al., 2012).

However, the LOC method has been shown to potentially overestimate the past variability. There is a comment and reply exchange on the Christiansen et al manuscript, and my interpretation of it is that Christian et al. also acknowledge that this could be a problem in certain circumstances.

Response: The sentence has been revised to "*The reconstructions based on the LOC method are assumed to better preserve the low-frequency climate signal compared to other methods, though they would overestimate the high-frequency signal (Christiansen and Ljungqvist, 2011).*", according to the reviewer's suggestion.

Item 10: 10 2.2 Tree-ring record

Please, be more specific here: three-ring width, isotopes, density, early wood density, etc.

Response: Following the reviewer's suggestion, we will add the metadata of all the proxy records in Table s1 in the revised manuscript.

Item 11: 11 To maximize the overlap lengths of the instrument data and proxy records, all treering records were extrapolated to AD 2000 using the RegEM algorithm

Extrapolation does not include new information and therefore it cannot increase the skill of the reconstructions. Was this step necessary for the OIE algorithm? if not, an explanation is required as to why the records were extrapolated.

Response: The extrapolation is necessary for the OIE method, because we used the correlation coefficient between the candidate proxy record and the reconstructed target to weight the candidate proxy records.

Item 12: 12 Discussion section. As I indicated in the preamble, this section actually contains further results, such as the superposed epoch analysis. It also contains the analysis of the link between the reconstructed precipitation and ENSO and the PDO. As it stands, it is a classical results section. The title' discussion' is misleading.

Response: Following the reviewer's suggestion, we have modified the structure of the paper and combined the results and discussion sections. We use thus the title 'Results and discussion'.

Item 13: 13. The superposed epoch analysis (SEA) between the precipitation, its PC1, and 35 large eruption events during AD 1470-1849 shows that volcanic activity as one important external forcing may affect the MJJAS precipitation anomalies variability for China (Fig. 8). Nevertheless, the signals are barely significant and there are similar averaged scores before and after the

These results are too cryptic. The SEA has not been mentioned before, so the reader is left wondering where this comes from: which eruptions have been included, how were they dated (the reconstructed volcanic forcing of Gao et al and of Crowley and Untermann does not always agree on the dating of the forcing maximum), how was the SEA itself conducted, for instance how many years prior to the eruptions were considered to define the pre-eruption mean, how was the statistical significance established, etc.

Response: Following the reviewer's suggestion, we have added the explanation of SEA method in the method section: "*The superposed epoch analysis (SEA) is traditionally used to analyse the influence of volcanic eruption on the climate, e.g., Bradley (1988). Here, the code to compute SEA has been downloaded from the website (http://blarquez.com/superposed-epoch-analysis-sea/). The period analysed (time window) are set as 20 years before and after each volcanic eruption event. The 90% confidence limit is estimated using the bootstrap procedure (Blarquez and Carcaillet, 2010). The eruption time series of Sigl et al. (2015) is used here because of the dating improvement compared to earlier estimates. Four categories of volcanic eruption events during the period from AD 1490 to AD 1829 are chosen following Zhuo et al. (2014)'s method which is based on the magnitude of their sulfate deposition in the Greenland ice-core records: (1) all Northern hemisphere eruption events (CNH0P)*

according to Sigl et al. (2015), (2) CNH1/2P: the eruption events that have more than half, (3) equal (CNH1P), and (4) double (CNH2P) that of the sulfate deposition of the 1991 Mount Pinatubo eruption.".

Moreover, we have updated Figure 8 as Figure s5 in the revised manuscript using the following Figure 1, which added the spatial patterns of the impact of the Northern Hemisphere volcanic eruption events on the precipitation field for the four categories of eruption (CNH0P, CNH1/2P, CNH1P, and CNH2P) of the volcanic events in Figure 1. *The SEA results applied to the mean precipitation anomalies (Fig. s5a), and its PC1 (Fig. s5b) during AD 1490-1829 shows that volcanic activity as one important external forcing might affect the MJJAS precipitation anomalies variability for China. Nevertheless, the signals are barely significant and there are similar averaged scores before and after the volcanic eruption year. Moreover, the spatial pattern of the impact of the Northern Hemisphere volcanic eruption events on the precipitation field (Figures s5c−f) is not consistent between the four categories of eruption (CNH0P, CNH1/2P, CNH1P, and CNH2P). This indicates that the response of MJJAS precipitation anomalies for China to Northern Hemispheric volcanic eruption is not robust.*
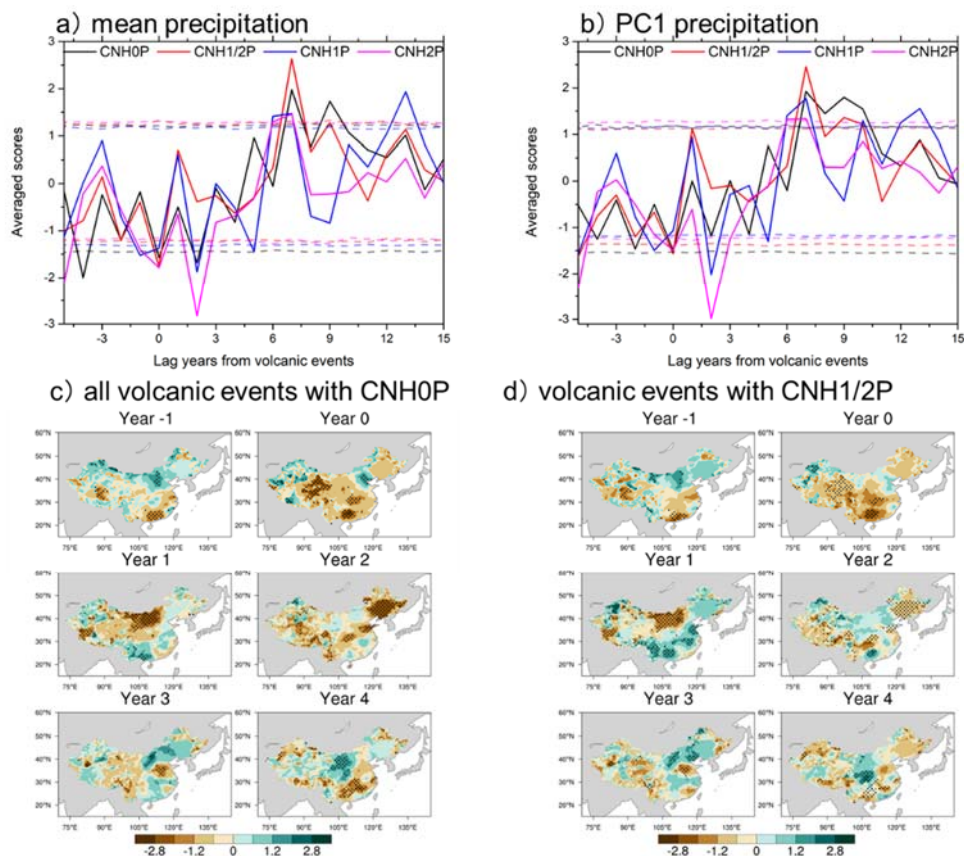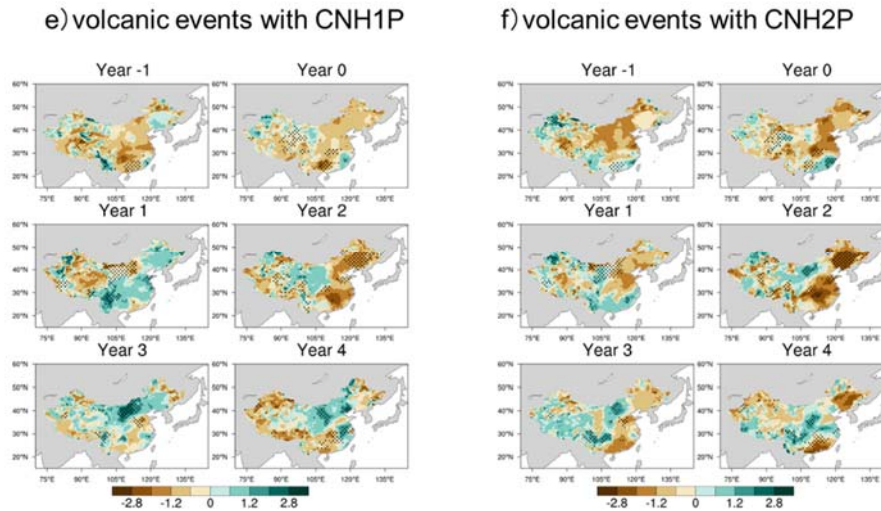
Figure 1 Superposed Epoch Analysis results applied to the mean precipitation anomalies (a), its PC1 (b), and the precipitation field (c-f) response to four categories (CNH0P, CNH1/2P, CNH1P, and CNH2P) of volcanic events as selected in Sigl et al. (2015) with 90% confidence limit during the period AD 1490-1829. The dashed lines in (a) and (b) are 90% confidence limit. The blank points in (c-f) identify statistically significant grid points at the 90% confidence level. The title of each panel in (c-f) indicates lag year from volcanic events.

Item 14: 14. Our results indicate thus that the south-north mode variability of precipitation anomalies in China carries very likely the fingerprint of ENSO evolution over the past 500 years, but the origin of the EOF1 and EOF3 patterns are not clearly established yet. This implies that the other factors such as North Atlantic Oscillation (NAO) (Wu et al., 2009; Zheng et al., 2016), interdecadal Pacific oscillation (IPO) (Song and Zhou, 2015), North Atlantic triple SST pattern (Ruan and Li, 2016) through the North Atlantic–Eurasia Teleconnection (AEAT) (Li et al., 2013a), the snow cover change of the Tibetan Plateau (Ding et al., 2009; Wu et al., 2012), and changes aerosol concentration (Li et al., 2016) may contribute to the reconstructed precipitation field modes during the pre-industrial period.

This conclusion is rather speculative. Why should EOF1 and EOF3 be related to the large-scale climate? they could be originated by regional processes in China.

Response: We agree with the reviewer's comment. This section is speculative but we wanted to include at this stage the reference to studies potentially useful to explain those patterns. Nevertheless, as we cannot explain the origins of EOF1 and EOF3 at the current stage, the regional processes in China is also a possible factor to affect them. Following the reviewer's suggestion, we have revised the part: "*Our results indicate thus that the south-north mode variability of precipitation anomalies in China carries very likely the fingerprint of ENSO evolution in tropical Pacific over the past 500 years. The origin of the EOF1 and EOF3 patterns is not clearly established yet, even though both of them maybe related to the western pacific subtropical high during the*

instrumental period (Wu and Wang, 2002). Moreover, some studies show that other factors such as the North Atlantic Oscillation (NAO) (Wu et al., 2009; Zheng et al., 2016) and the North Atlantic triple SST pattern (Ruan and Li, 2016), the interdecadal Pacific oscillation (IPO) (Song and Zhou, 2015), the snow cover change of the Tibetan Plateau (Ding et al., 2009; Wu et al., 2012), and some regional processes in China may contribute to the precipitation field modes during the instrumental period. Thus, additional studies are then required to determine which of these processes might be related to EOF1 and EOF3 over the pre-industrial period.".

Item 15: 15. Caption Figure 1. Please indicate what RSQ, RE, CE and uncertainty mean

Response: Following the reviewer's suggestion, we have added the full names of these terms in the caption of Figure 3, like as "*The r^2 is the square of the Pearson product–moment correlation coefficient, the RE and CE are the reduction of error and the coefficient of efficiency, the uncertainty is characterized from the standard deviation of the residual between the reconstructed and instrumental precipitation data during the verification period.*" Moreover, we have added some words to explain these terms in the method section, like as "*Traditional accuracy and skill parameters, including the square of the Pearson product–moment correlation coefficient (r^2) between the reconstruction and the instrumental data during the verification period, the reduction of error (RE) in the verification period, and the coefficient of efficiency (CE) in the verification period (Cook et al., 2010), were used to evaluate the reliability of the reconstructions, and the uncertainty was calculated using the standard deviation of the residual between the reconstructed and instrumental precipitation data during the verification period.. The significance of the correlation for the filtered time series was accessed using the effective number of degrees of freedom following Zhao et al. (2016).*"

References

Bradley, R. S.: The explosive volcanic eruption signal in Northern Hemisphere continental temperature records, Clim. Chang., 221-243, doi:10.1007/BF00139431, 1988.

Christiansen, B.: Reconstructing the NH mean temperature: Can underestimation of trends and variability be avoided? J. Climate, 24, 674-692, doi:10.1175/2010jcli3646.1, 2011.

Christiansen, B., and Ljungqvist, F. C.: Reconstruction of the extratropical NH Mean temperature over the last millennium with a method that preserves low-frequency variability, J. Climate, 24, 6013-6034, doi:10.1175/2011jcli4145.1, 2011.

Christiansen, B., and Ljungqvist, F. C.: Challenges and perspectives for large-scale temperature reconstructions of the past two millennia, Rev. Geophys., 55, 40-96, doi:10.1002/2016RG000521, 2017.

Cook, E. R., Meko, D. M., Stahle, D. W., and Cleaveland, M. K.: Drought reconstructions for the continental United States, J. Climate, 12, 1145-1162, doi:10.1175/1520-0442(1999)012<1145:DRFTCU>2.0.CO;2, 1999.

Ding, Y., Sun, Y., Wang, Z., Zhu, Y., and Song, Y.: Inter-decadal variation of the summer precipitation in China and its association with decreasing Asian summer monsoon Part II: Possible causes, Int. J. Climatol., 29, 1926-1944, doi:10.1002/joc.1759, 2009.

Evans, M., Kaplan, A., Cane, M., and Villalba, R.: Chapter 4 – Globality and optimality in climate field reconstructions from proxy data, in: Interhemispheric climate linkages, ed. Vera Markgraf., Academic Press, San Diego, 53-72, doi:10.1016/B978-012472670-3/50007-0, 2001.

Gómez-Navarro, J. J., Werner, J., Wagner, S., Luterbacher, J., and Zorita, E.: Establishing the skill of climate field reconstruction techniques for precipitation with pseudoproxy experiments, Clim. Dyn., 45, 1395-1413, doi:10.1007/s00382-014-2388-x, 2015.

Hanhijärvi, S., Tingley, M., and Korhola, A.: Pairwise comparisons to reconstruct mean temperature in the Arctic Atlantic Region over the last 2,000 years, Clim. Dyn., 41, 2039-2060, doi:10.1007/s00382-013-1701-4, 2013.

Mann, M. E., Bradley, R. S., and Hughes, M. K.: Northern hemisphere temperatures during the past millennium: Inferences, uncertainties, and limitations, Geophys. Res. Lett., 26, 759-762, 1999.

Mann, M. E., Zhang, Z. H., Hughes, M. K., Bradley, R. S., Miller, S. K., Rutherford, S., and Ni, F. B.: Proxy-based reconstructions of hemispheric and global surface temperature variations over the past two millennia, Proc. Nat. Acad. Sci. U.S.A., 105, 13252-13257, doi:10.1073/pnas.0805721105, 2008.

Mann, M. E., Zhang, Z. H., Rutherford, S., Bradley, R. S., Hughes, M. K., Shindell, D., Ammann, C., Faluvegi, G., and Ni, F. B.: Global Signatures and Dynamical Origins of the Little Ice Age and Medieval Climate Anomaly, Science, 326, 1256-1260, doi:10.1126/science.1177303, 2009.

McShane, B. B., and Wyner, A. J.: A statistical analysis of multiple temperature proxies: Are reconstructions of surface temperatures over the last 1000 years reliable? Ann. Appl. Stat., 5, 5-44, DOI: 10.1214/10-AOAS398, 2011.

Neukom, R., Luterbacher, J., Villalba, R., Kuttel, M., Frank, D., Jones, P. D., Grosjean, M., Wanner, H., Aravena, J. C., Black, D. E., Christie, D. A., D'Arrigo, R., Lara, A., Morales, M., Soliz-Gamboa, C., Srur, A., Urrutia, R., and von Gunten, L.: Multiproxy summer and winter surface air temperature field reconstructions for southern South America covering the past centuries, Clim. Dyn., 37, 35-51, doi:10.1007/s00382-010-0793-3, 2011.

Ruan, C., and Li, J.: An improvement in a time-scale decomposition statistical downscaling prediction model for summer rainfall over North China. Chin. J. Atmos. Sci., 40, 215-226, doi:10.3878/j.issn.1006-9895.1503.14317, 2016. (in Chinese)

Shi, F., Yang, B., Charpentier Ljungqvist, F., and Yang F.: Multi-proxy reconstruction of Arctic summer temperatures over the past 1400 years, Clim. Res., 54, 113-128, doi:10.3354/cr01112, 2012.

Shi, F., Ge, Q., Yang, B., Li, J., Yang, F., Ljungqvist, F. C., Solomina, O., Nakatsuka, T., Wang, N., Zhao, S., Xu, C., Fang, K., Sano, M., Chu, G., Fan, Z., Narayan, P. G., and Muhammad, U. Z.: A multi-proxy reconstruction of spatial and temporal variations in Asian summer temperatures over the last millennium Clim. Chang., 131, 663-676, doi:10.1007/s10584-015-1413-3, 2015a.

Sigl, M., Winstrup, M., McConnell, J. R., Welten, K. C., Plunkett, G., Ludlow, F., Buntgen, U., Caffee, M., Chellman, N., Dahl-Jensen, D., Fischer, H., Kipfstuhl, S., Kostick, C., Maselli, O. J., Mekhaldi, F., Mulvaney, R., Muscheler, R., Pasteris, D. R., Pilcher, J. R., Salzer, M., Schupbach, S., Steffensen, J. P., Vinther, B. M., and Woodruff, T. E.: Timing and climate forcing of volcanic eruptions for the past 2,500 years, Nature, 523, 543-549, doi:10.1038/nature14565, 2015.

Song, F., and Zhou, T.: The crucial role of internal variability in modulating the decadal variation of the East Asian summer monsoon–ENSO relationship during the twentieth century, J. Climate, 28, 7093-7107, 2015.

Tingley, M. P., and Huybers, P.: A Bayesian Algorithm for Reconstructing Climate Anomalies in Space and Time. Part I: Development and Applications to Paleoclimate Reconstruction Problems, J. Climate, 23, 2759-2781, doi:10.1175/2009jcli3015.1, 2010.

Wu, Z., Wang, B., Li, J., and Jin, F.: An empirical seasonal prediction model of the East Asian summer monsoon using ENSO and NAO, J. Geophys. Res. [Atmos.], 114, D18120, doi:10.1029/2009JD011733, 2009.

Wu, Z., Li, J., Jiang, Z., and Ma, T.: Modulation of the Tibetan Plateau snow cover on the ENSO teleconnections: From the East Asian summer monsoon perspective, J. Climate, 25, 2481-2489, doi:10.1175/JCLI-D-11-00135.1, 2012.

Yang, F., Wang, N., Shi, F., Ljungqvist, F. C., Wang, S., Fan, Z., and Lu, J.: Multi-proxy temperature reconstruction from the West Qinling Mountains, China, for the past 500 years, PLoS ONE, 8, e57638, doi:10.1371/journal.pone.0057638, 2013b.

Yang, F., Wang, N., Shi, F., Ljungqvist, F. C., Zhao, S., and Liu, T.: The spatial distribution of precipitation over the West Qinling region, China, AD 1470–2000, Palaeogeogr. Palaeoclimatol. Palaeoecol., 443, 278-285, doi:10.1016/j.palaeo.2015.12.003, 2016.

Zheng, F., Li, J., Li, Y., Zhao, S., and Deng, D.: Influence of the summer NAO on the spring-NAO-based predictability of the East Asian summer monsoon, J. Appl. Meteorol. Climatol., doi:10.1175/JAMC-D-15-0199.1, 2016.

Zhuo, Z., Gao, C., and Pan, Y.: Proxy evidence for China's monsoon precipitation response to volcanic aerosols over the past seven centuries, J. Geophys. Res. [Atmos.], 119, 6638-6652, doi:10.1002/2013JD021061, 2014.

II.   Response to reviewer 2:

General comments:

This is an interesting paper which introduces a newly generated annual warm season precipitation reconstruction over China. The reconstruction is based on the point-to-point regression-based method and a dense data network including 489 tree-ring width data, 2 tree-ring isotope data, 108 drought/flood index, and 1 long-term instrumental data. The verification results show good agreements between the reconstruction and instrumental data over eastern China. The paper is in itself interesting, but its structure and language needs to be improved. Since the methodologies have been commented by another reviewer, here I mainly add some comments about the proxy records.

Response: We would like to thank the reviewer for his/her constructive review, comments, and suggestions, which have helped us to greatly improve our manuscript. We have done our best to address the reviewer's concerns and modified the manuscript in light of the reviewer's suggestions, in particular to improve the structure and the language. Point-by-point responses to the reviewer's comments are listed below.

Major comments:

Item 1: 1. "Each record is required to be significantly correlated with one or more instrumental precipitation record at the 90% (p < 0.1) confidence level during the overlap period, based on both raw data and linearly detrended data."

How did you do the correlation analysis? How many nearby instrumental grid cells did you compare the proxy data with? It is surprising that all 489 tree-ring proxy records are "sensitive precipitation proxy records ".

Response: We calculated the Pearson's linear correlation coefficient between the targeted precipitation grid point and the candidate tree-ring record which is located in the range of the search radius, and select all tree-ring records that are positively and significantly related with one instrumental precipitation grid points during the period AD 1961-2000 at least (r > 0 and p < 0.1). Figure 1 shows the number of grid points that is reconstructed using each tree-ring record. e.g. a tree-ring record with "100" value means that it has significant relationship with 100 nearby instrumental precipitation grid points. This illustrates that all tree-ring records are significantly related to a precipitation grid point at least.

Thanks to your question, we have revised this statement, it is '*proxy records that can be significantly related to precipitation in the domain studied*' not '*sensitive precipitation proxy records*', because we do not determine whether the precipitation is the major limit factor of tree-ring width chronology and use all possible predictors to extend the spatial coverage.
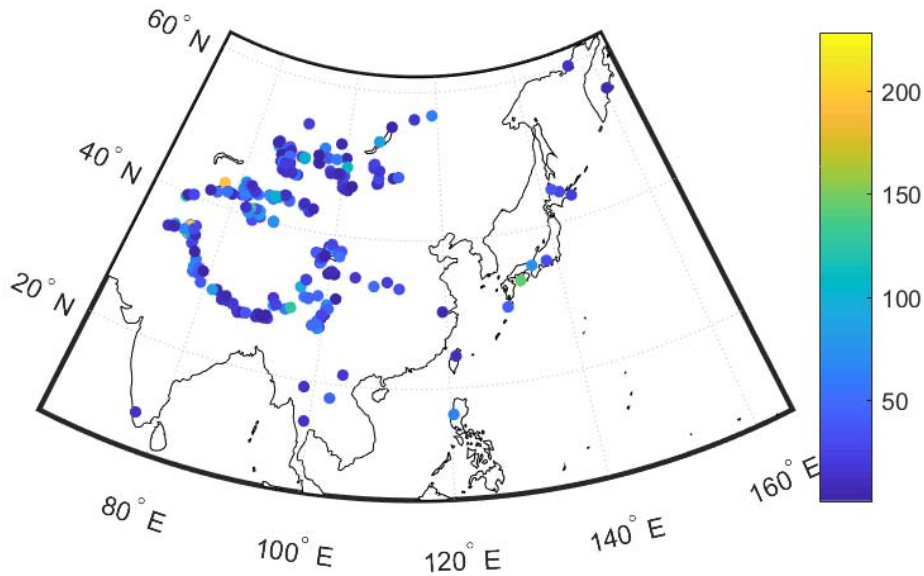
Figure 1 The number of grid points which is reconstructed using each tree-ring record.

Item 2: 2. The quality of DWI before the instrumental period needs to be discussed.

Response: Following the reviewer's suggestion, we have added two Figures 2, 3 and a discussion on the quality of DWI in the revised manuscript, like as "*The DWI dataset is mainly derived from the local chronicles and started from 1470 (the sixth Year of Cheng hua reign in Ming Dynasty), which describe the onset, duration, areal extent, and severity of each drought or flood event in each province, China (Chinese Academy of Meteorological Science, 1981; Zhang, 1983). The experts, mainly from the provincial meteorological bureau provinces, China Meteorological Administration, Peking University, and Chinese Academy of Sciences, converted qualitative textual descriptions into quantitative data (Chinese Academy of Meteorological Science, 1981).*

The reliability of DWI was described in previous studies (Zhang, 1983; Zhang, 1988), e.g., the homogeneity of DWI was demonstrated using the chi-square test (Zhang, 1983), and the reliability of DWI in spatial pattern was verified through comparison with the eigenvectors of the instrumental precipitation during the period AD 1951-1974 (Wang and Zhao, 1979).

However, DWI have still some weaknesses. The first one is time discontinuity (Zhang, 1983). Figure s1 is the time spans of 107 DWI records. This illustrates that most of DWI records are not continuous in time. The maximum (mean) number of missing values of 107 DWI records during the period AD 1470-2000 was 446 (157). Secondly, the DWI is unevenly distributed over space. Figure s2 shows that the location and number of DWI records during the period AD 1470-2000. On this figure, a value of "100" means that it has 100 observed values during the period AD 1470-2000. It indicates that 91 of 107 DWI records are located in eastern China (east of longitude 105°E), which is the economically developed region. There are only 16 DWI records west of longitude 100°E. Additionally, an uncertainty due to the subjective judgment is unavoidable for the

historical documentary, even though the different sources have been used to cross-validate the final reconstruction (Zhang, 1983; Man, 2009; Ge, 2011; Zheng et al., 2014a). Moreover, the range of values is within five grades and the DFI record is not an accurate precipitation value, thus it also limits the accuracy and ability to detect the extreme events (Zheng et al., 2014a).
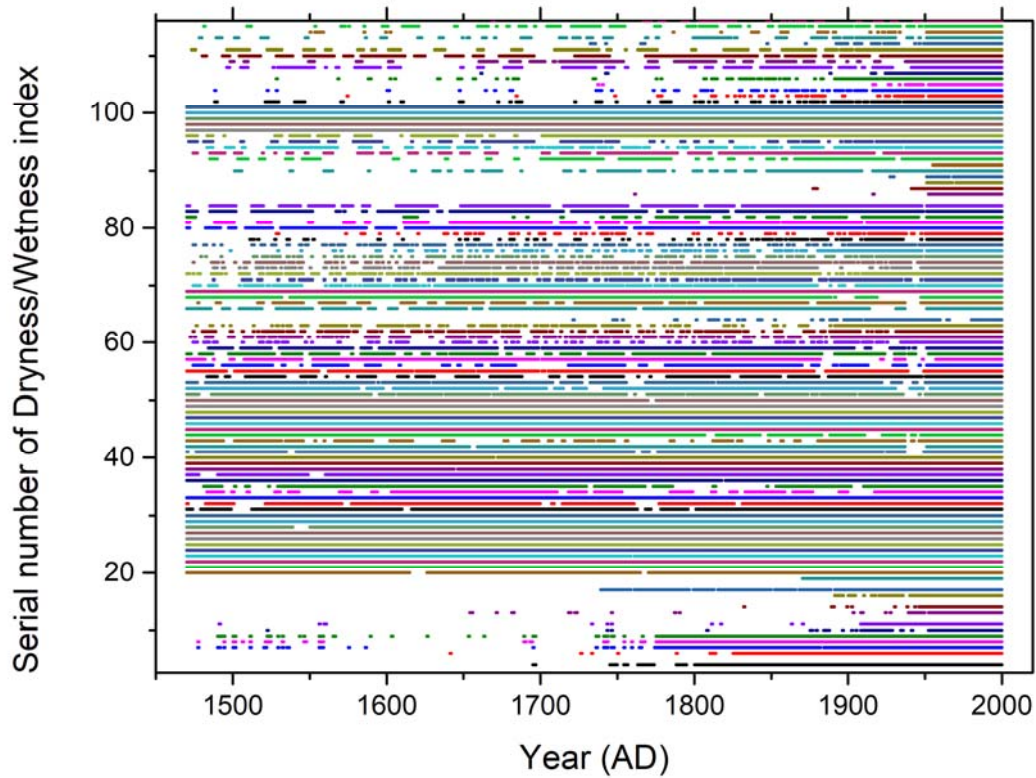

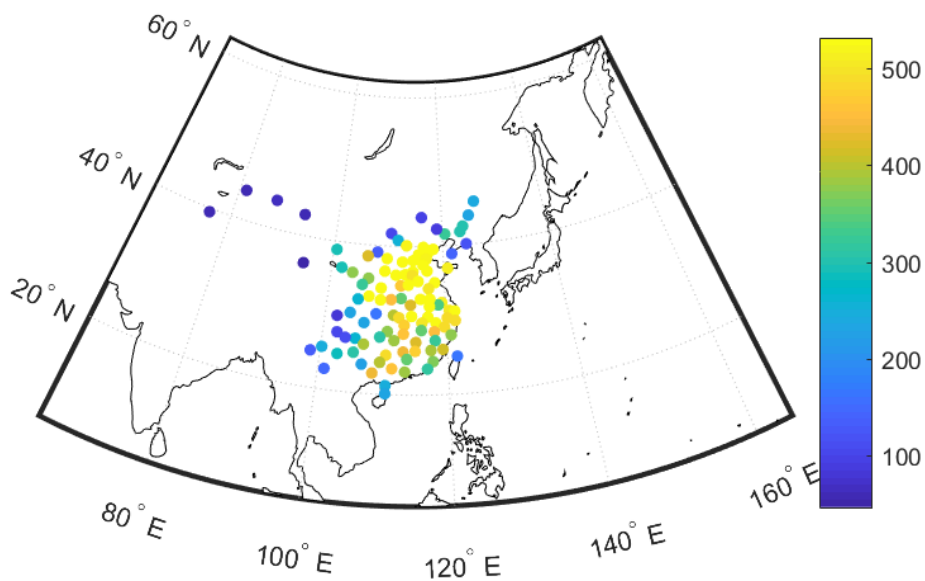Figure 2 The time span of each Dryness/Wetness index.

Figure 3 The number of observation of each Dryness/Wetness index during the period AD 1470-2000.

In order to improve the quality of the DWI dataset, Professor Zhang De'er lead a team of scientists, that carried out research during 20 years to identify the weather events in China over the past 3000 years. This resulted in the publication of a book, entitled "A compendium of Chinese meteorological records of the last 3,000 years". Each record has been carefully cross-checked from more than 8,000 historical documents (Zhang, 2004). However, the updated dataset is not archived in publish repository so far."

Item 3: 3. As you mentioned the precipitation/ PDSI reconstructions over East Asia from Cook et al. (2010) and Feng et al. (2013), have you compared this reconstruction with theirs?

Response: Following the reviewer's suggestion, we have calculated the correlation between Cook's PDSI reconstruction (Cook et al., 2010) with our precipitation reconstruction in Figure 4.

Figure 4 shows that the spatial correlation between them. We have included Figure 4 as supplementary material and discussed it in the revised manuscript, like as "*Strong correlations appear in the northeastern Tibetan Plateau, where there are longest and most abundant tree-ring width chronologies in China. Here, the precipitation is possibly a primary control factor of the tree-ring width chronology (Zhang et al., 2003c; Yang et al., 2014b). There are weak correlations between the reconstructions in eastern China even through the correlation coefficients are significant in some regions. The MADA is not consistent with the DWI records in eastern China, since only very few and short tree-ring width chronologies in eastern China are used to reconstruct the MADA (Yang et al., 2013a; Kang et al., 2014; Yang et al., 2014a; Zheng et al., 2014b; Ge et al., 2016).*"
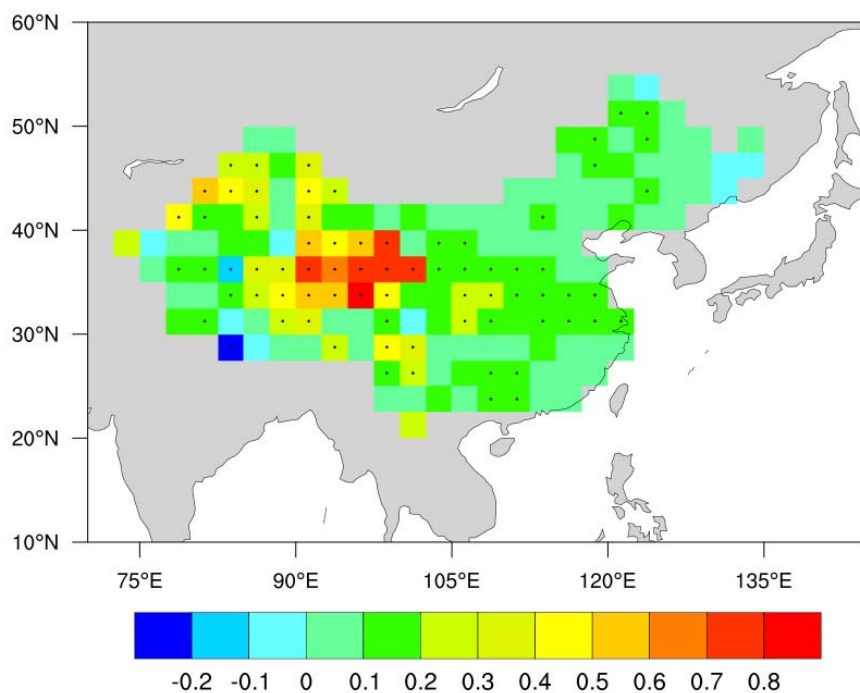
Figure 4 Spatial correlation between the PDSI reconstruction (Cook et al., 2010) and the precipitation field reconstruction obtained in this study. The dark spots mean the significant levels of the correlation coefficients at the 99% confidence level.

It is a pity that the precipitation reconstruction (Feng et al., 2013) is not achieved in any published database. However, we have added Figure 5 as Figure 6 in the revised manuscript for qualitative comparison of five historical Chinese droughts.

The selection of five drought periods follows Feng et al. (2013) but the spatial patterns in our reconstruction display some clear differences from their results. A "north drought with south flooding" dipole pattern in eastern China is seen in Figures 6a−d, and there is a triple pattern in eastern China in Fig. 6e. A similar dipole pattern can be found in Figures 5b and 5d (Feng et al., 2013) for two drought events (AD 1586−89 and AD 1876−78) but during four out of five drought periods, most of northeastern China is relatively humid situation in our study, which is not consistent with Feng et al. (2013)'s Fig. 5. An exceptional drought condition in northeastern China appears in the 1876-1878 drought event, which is the most severe drought of five events in eastern China.
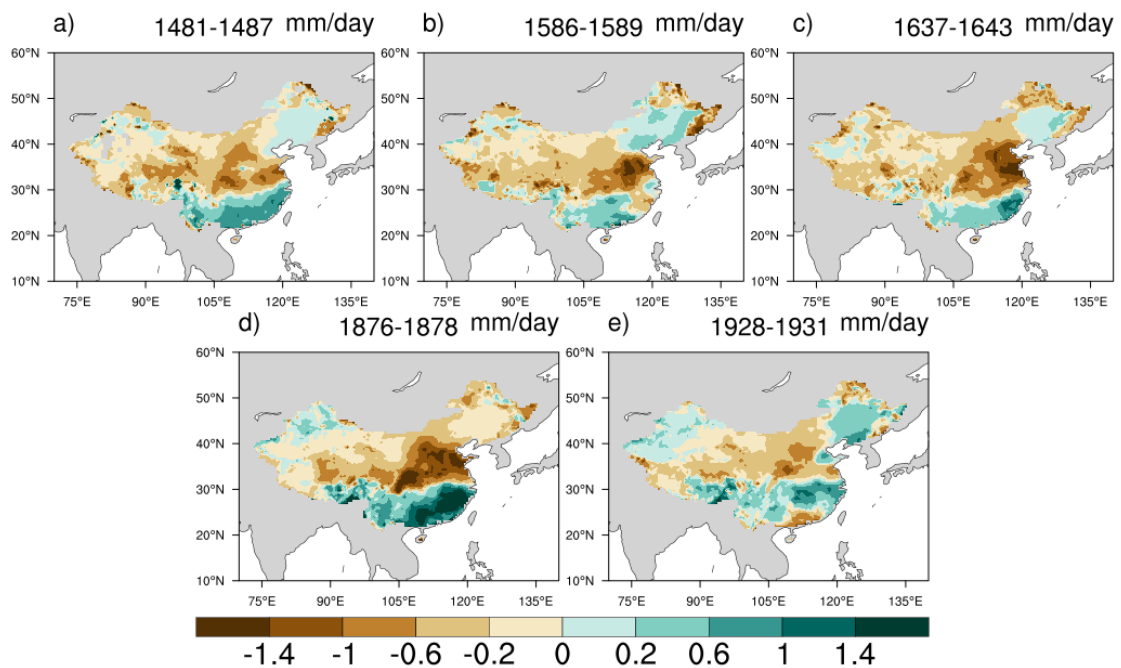

Figure 5 Spatial patterns of the May–September precipitation field relative to the 1961–90 climatological mean during five severe droughts in China.

Moreover, the reconstruction skills are low in semiarid and arid regions (Feng et al., 2013), because there are very few tree-ring chronologies in Western China in that reconstruction. We used some tree-ring width chronologies in Western China to compensate this weakness.

Item 4: 4. "A total of 242 of 491 tree-ring chronologies were extrapolated. The maximum and mean extrapolation lengths of the 242 chronologies were 24 years and

As you mentioned "all tree-ring records were extrapolated to AD 2000", that means lots of infilling data are between 1981-2000CE, which overlaps with the calibration period (1981-2000CE). Have you considered using a longer calibration period and leave out the last ten years?

Response: The extrapolation is necessary for the OIE method, because we used the correlation coefficient between the candidate proxy record and the reconstructed target to weight the candidate proxy records. Following the reviewer's suggestion, we have used a longer calibration period (1961-1990) and the last ten years as the verification period (1991-2000). The corresponding contents have revised according to the updated results.

Item 5: The second and third leading EOF patterns, the south-north dipole and the sandwich triple pattern, are indeed found in instrumental period. And they are closely related to the movement and intensity of the western pacific subtropical high (WPSH). The sea surface temperature can influence the rainfall through WPSH, but correlation maps between ENSO and summer precipitation are often noisy (Wu and Wang 2002). So, why would the signal of ENSO in rainfall be so strong in the reconstructions if it is noisy in instrumental rainfall data?

Response: This is indeed an interesting point. We have calculated the running correlation between the 17 reconstructed ENSO indices and the precipitation anomalies averaged over Yangtze River region and Huai River region in Figures 6a-b. We have followed Wu and Wang (2002) for the region definition. All data were filtered to obtain the interannual components when calculating running correlation coefficients using the Ensemble Empirical mode decomposition (EEMD) method, because the ENSO variability is in the interannual 3–7 year period band (Trenberth, 1997). Results indicate that the relationship between ENSO and summer precipitation in China are not stable in the reconstructions, which is consistent with the instrumental period (Wu and Wang, 2002). However, we have calculated the correlation coefficient between the 17 ENSO indices and the precipitation for the full period, and all show that small and positive correlation. Thus, a more robust link between ENSO and summer precipitation in China may be found, if we analyze the full period. Moreover, the explanatory variance of the second dominant mode of precipitation is only about 11.2%. This indicates that different factors may substantially affect the spatial pattern of the precipitation field, e.g. the snow cover change of the Tibetan Plateau (Ding et al., 2009).

Finally, we have added the statement that the two leading EOF patterns are closely related to the western pacific subtropical high (Wu and Wang, 2002) in the revised manuscript, like as "*The origin of the EOF1 and EOF3 patterns over the pre-industrial period is not clearly established yet, even though both of them maybe related to the movement and intensity of the western pacific subtropical high during the instrumental period (Wu and Wang, 2002).*".
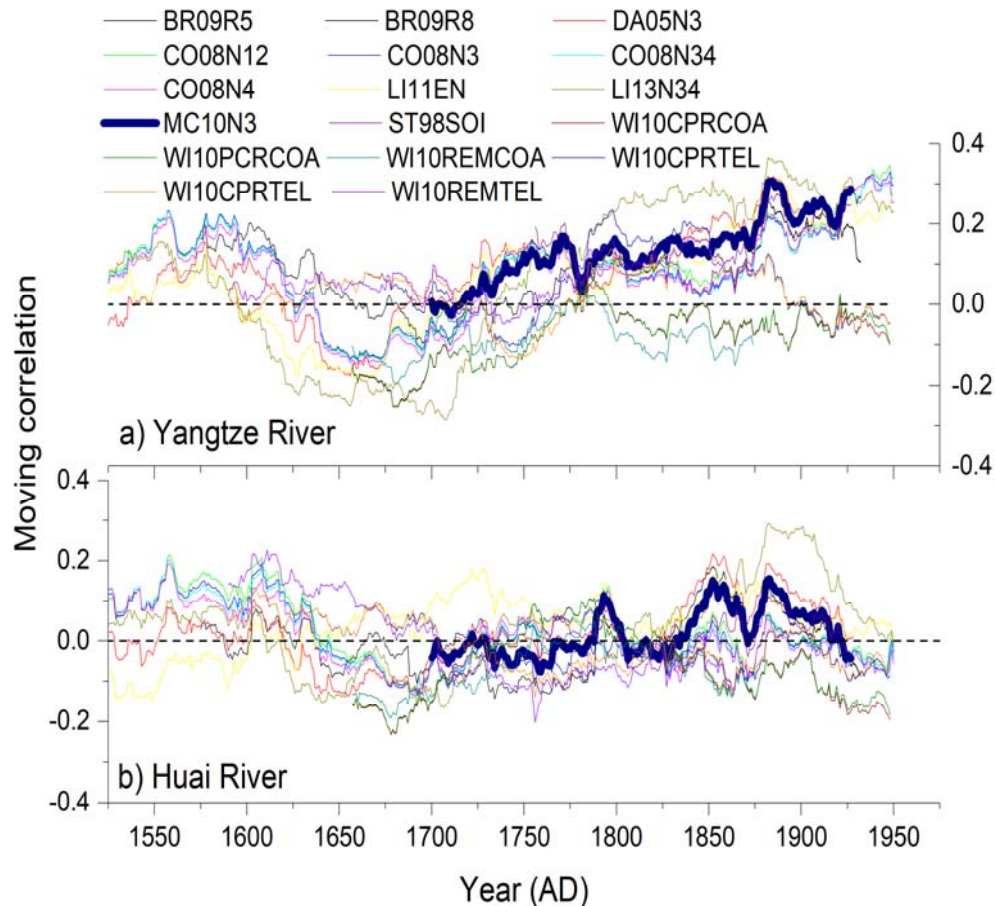
Figure 6 The 101-year running correlation coefficients of the interannual components of 17 ENSO indices with the reconstructed precipitation anomalies averaged over Yangtze River region (28°−32°N, 110°−120°E; a) and Huai River region (32.5°−35.5°N, 115°−120°E; b). The interannual components were obtained using the Ensemble Empirical mode decomposition (EEMD) method.

Item 6: 6. In Figure 9, which method did you use for the correlation analysis? How does it look using winter temperature in the Nino 3.4 region?

Response: In Figure 9, the Pearson's sample linear cross-correlations at lag 0 is used for the correlation analysis, and the effective number of degrees of freedom is calculated following Zhao et al. (2016) to access the significance of the correlation. The unified ENSO proxy (UEP) (McGregor et al., 2010) is used to calculate the relationship between the precipitation field and the ENSO index. This index is the first PC of ten reconstructed ENSO indices, and is scaled to the instrumental HadSST1 annual mean (July–June) Niño 3.4 region sea surface temperature anomalies (McGregor et al., 2010). We have added this explanation in the method section. Moreover, we have calculated the relationship between the previous winter (December–January–February) Niño 3.4 index and the precipitation field for each model in Figure 7, which is added as Figure s7 in the revised manuscript. The spatial pattern is very similar with the result of annual mean Niño 3.4 index.
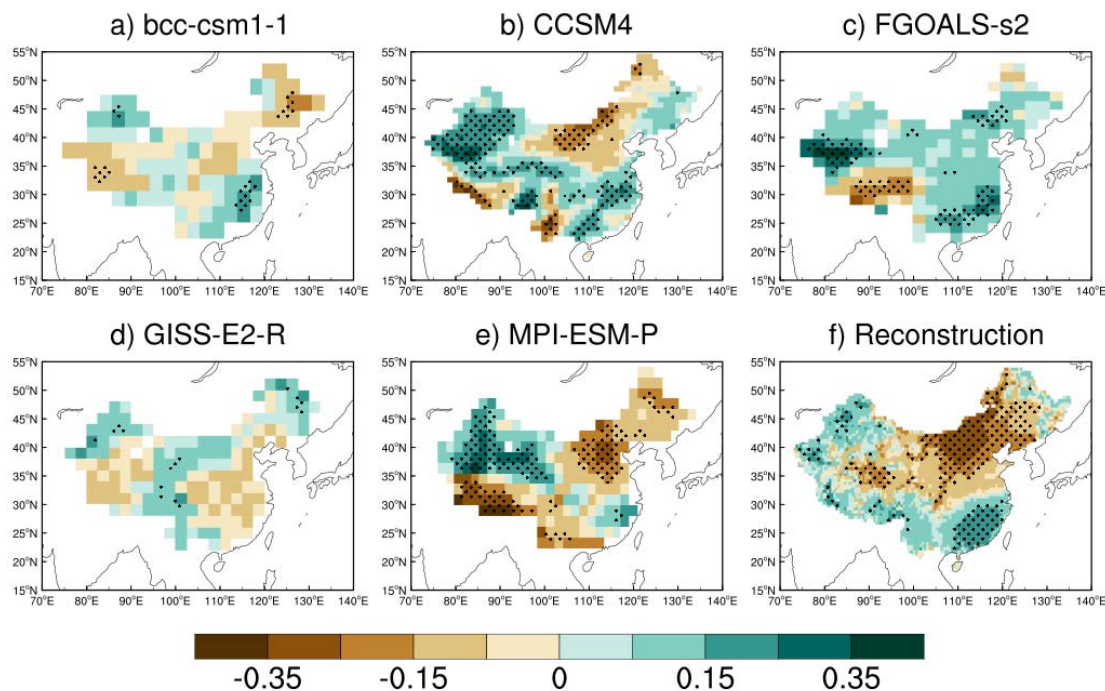
Figure 7 (a-e) Correlation maps of simulated MJJAS mean precipitation anomalies for China with the corresponding simulated preceding winter (DJF) Niño 3.4 index in five different models (bcc-csm1-1, CCSM4, FGOALS-s2, GISS-E2-R, and MPI-ESM-P). (f) Correlation maps of reconstructed MJJAS mean precipitation anomalies for China with a reconstructed annual mean ENSO index from McGregor et al. (2010).

References

Cook, E. R., Anchukaitis, K. J., Buckley, B. M., D'Arrigo, R., Jacoby, G. C., and Wright, W. E.: Asian monsoon failure and megadrought during the last millennium, Science, 328, 486-489, doi:10.1126/science.1185188, 2010.

Ding, Y., Wang, Z., and Sun, Y.: Inter-decadal variation of the summer precipitation in East China and its association with decreasing Asian summer monsoon. Part I: Observed evidences, Int. J. Climatol., 28, 1139-1161, doi:10.1002/joc.1615, 2008.

Ding, Y., Sun, Y., Wang, Z., Zhu, Y., and Song, Y.: Inter-decadal variation of the summer precipitation in China and its association with decreasing Asian summer monsoon Part II: Possible causes, Int. J. Climatol., 29, 1926-1944, doi:10.1002/joc.1759, 2009.

Feng, S., Hu, Q., Wu, Q., and Mann, M. E.: A gridded reconstruction of warm season precipitation for Asia spanning the past half millennium, J. Climate, 26, 2192-2204, doi:10.1175/jcli-d-12-00099.1, 2013.

Ge, Q.: The climate change in China during the past dynasties, Science Press, Beijing, 2011. (in Chinese)

Ge, Q., Zheng, J., Hao, Z., Liu, Y., and Li, M.: Recent advances on reconstruction of climate and extreme events in China for the past 2000 years, J. Geog. Sci., 26, 827-854, doi:10.1007/s11442-016-1301-4, 2016.

Kang, S., Bräuning, A., and Ge, H.: Tree-ring based evidence of the multi-decadal climatic oscillation during the past 200 years in north-central China, J. Arid Environ., 110, 53-59, doi:10.1016/j.jaridenv.2014.06.003, 2014.

Li, Z., Lau, W. K. M., Ramanathan, V., Wu, G., Ding, Y., Manoj, M. G., Liu, J., Qian, Y., Li, J., Zhou, T., Fan, J., Rosenfeld, D., Ming, Y., Wang, Y., Huang, J., Wang, B., Xu, X., Lee, S. S., Cribb, M., Zhang, F., Yang, X., Zhao, C., Takemura, T., Wang, K., Xia, X., Yin, Y., Zhang, H., Guo, J., Zhai, P. M., Sugimoto, N., Babu, S. S., and Brasseur, G. P.: Aerosol and monsoon climate interactions over Asia, Rev. Geophys., 54, 866-929, doi:10.1002/2015RG000500, 2016.

Man, Z.: Climatic change historical period of China, Shandong Education Press, Jinan, 2009. (in Chinese)

McGregor, S., Timmermann, A., and Timm, O.: A unified proxy for ENSO and PDO variability since 1650, Clim. Past, 6, 1-17, doi:10.5194/cp-6-1-2010, 2010.

Trenberth, K. E.: The definition of el nino, Bull. Am. Meteorol. Soc., 78, 2771-2777, 1997.

Wu, R., and Wang, B.: A Contrast of the East Asian Summer Monsoon–ENSO Relationship between 1962–77 and 1978–93, J. Climate, 15, 3266-3279, doi:10.1175/1520-0442(2002)015<3266:ACOTEA>2.0.CO;2, 2002.

Yang, B., Kang, S., Ljungqvist, F. C., He, M., Zhao, Y., and Qin, C.: Drought variability at the northern fringe of the Asian summer monsoon region over the past millennia, Clim. Dyn., 43, 845-859, doi:10.1007/s00382-013-1962-y, 2014a.

Yang, B., Qin, C., Wang, J., He, M., Melvin, T. M., Osborn, T. J., and Briffa, K. R.: A 3,500-year tree-ring record of annual precipitation on the northeastern Tibetan Plateau, Proc. Nat. Acad. Sci. U.S.A., 111, 2903-2908, doi:10.1073/pnas.1319238111, 2014b.

Yang, F., Shi, F., Kang, S., Wang, S., Xiao, Z., Nakatsuka, T., and Shi, J.: Comparison of the dryness/wetness index in China with the Monsoon Asia Drought Atlas, Theor. Appl. Climatol., 114, 553-566, doi:10.1007/s00704-013-0858-4, 2013a.

Zhang, D.: Method to reconstruct climatic series for the past 500 years and its reliability, Collected Papers of Meteorological Science and Technology, 4, 17-26, 1983. (in Chinese)

Zhang, D.: The method for reconstruction of the dryness/wetness series in China for the last 500 years and its reliability, in: Zhang, J. (ed): The reconstruction of climate in China for historical times. Science Press, Beijing, China, 18-30, 1988.

Zhang, D.: A compendium of Chinese meteorological records of the last 3000 years, Nanjing: Jiangsu Education Publishing House, 2004. (in Chinese)

Zhang, Q., Cheng, G., Yao, T., Kang, X., and Huang, J.: A 2,326-year tree-ring record of climate variability on the northeastern Qinghai-Tibetan Plateau, Geophys. Res. Lett., 30, 1739-1742, doi:10.1029/2003gl017425, 2003c.

Zhao, S., Li, J., and Sun, C.: Decadal variability in the occurrence of wintertime haze in central eastern China tied to the Pacific Decadal Oscillation, Sci. Rep., 6, 27424, doi:10.1038/srep27424, 2016.

Zheng, J., Ge, Q., Hao, Z., Liu, H., Man, Z., Hou, Y., and Fang, X.: Paleoclimatology proxy recorded in historical documents and method for reconstruction on climate change, Quat. Sci., 34, 1186-1196, doi:10.3969/j.issn.1001-7410.2014.06.07, 2014a. (in Chinese)

Zheng, J., Hao, Z., Fang, X., and Ge, Q.: Changing characteristics of extreme climate events during past 2000 years in China, Prog. in Geogr., 33, 3-12, doi:10.11820/dlkxjz.2014.01.001, 2014b. (in Chinese)

Multi-proxy reconstructions of <u>May–September</u> precipitation field in China over the past 500 years

Feng Shi[1,2*], Sen Zhao[3,4], Zhengtang Guo[1,5,6], Hugues Goosse[2]<u>, Qiuzhen Yin[2]</u>

[1]Key Laboratory of Cenozoic Geology and Environment, Institute of Geology and Geophysics, Chinese Academy of Sciences, Beijing, 100029, China

[2]Georges Lemaître Centre for Earth and Climate Research, Earth and Life Institute, Université catholique de Louvain, Louvain-la-Neuve, 1348, Belgium

[3]Key Laboratory of Meteorological Disaster of Ministry of Education, and College of Atmospheric Science, Nanjing University of Information Science and Technology, Nanjing, 210044, China

[4]School of Ocean and Earth Sciences and Technology, University of Hawaii at Mānoa, Honolulu, HI, 96822, USA

[5]CAS Center for Excellence in Tibetan Plateau Earth Sciences, Beijing, 100101, China

[6]University of Chinese Academy of Sciences, Beijing, 100049, China

Correspondence to: Feng SHI (shifeng@mail.iggcas.ac.cn)

Abstract. The dominant modes of variability of precipitation for the whole ~~of~~ China over the past millennium and the mechanism governing their spatial structure remain unclear. The first reason is probably that it is difficult to reconstruct the precipitation field in western China because the published high-resolution proxy records for this region are scarce. Numerous tree-ring chronologies have recently been archived in publicly available databases through PAGES2k activities, and these provide an opportunity to refine precipitation field reconstructions for China. Based on ~~600~~ <u>479</u> proxy records, including ~~491~~ <u>371</u> tree-ring <u>width</u> chronologies, <u>a tree-ring isotope chronology, and</u> ~~108~~ <u>107</u> drought/flood indices~~, and a long-term instrumental precipitation record from South Korea~~, we <u>reconstruct</u>~~revised~~ the precipitation field ~~reconstruction~~ for China for the past half millennium using the optimal information extraction method. A total of <u>3631</u>~~3971~~ of 4189 grid points in the reconstruction field passed the cross-validation process, accounting for ~~94.8~~<u>86.68</u>% of the total number of grid points. The first leading mode of variability of the reconstruction shows coherent variations over most of China. The second mode, a north–south dipole in eastern China with variations of the same sign in western China and <u>northern</u>~~southeastern~~ China, <u>except for Xinjiang province,</u> may be controlled by the El Niño-Southern Oscillation (ENSO) variability. The third mode, a "sandwich" triple mode in eastern China with variations of the same sign in western China and central China. Five of the six coupled ocean-atmosphere climate models (BCC-CSM1.1, CCSM4, FGOALS-s2, GISS-E2-R and MPI-ESM-P) of the

Paleoclimate Modeling Intercomparison Project Phase III (PMIP3), can reproduce the south-north dipole mode of precipitation in eastern China, and its likely link with ENSO. However, there is mismatch in terms of their time development. This is consistent with an important role of the internal variability in the precipitation field changes over the past 500 years.

1 Introduction

High-resolution regional paleoclimate field reconstructions are able to accurately reproduce the fine spatiotemporal structure of regional climate change on multiple timescales for the period prior to instrumental records. Such reconstructions are an essential source of information to document the climate variability at decadal to centennial time scales and can be used to assess the ability of climate models to simulate past climate change.

In order to obtain such a reconstruction of regional paleoclimate fields, dense proxy records and an adequate reconstruction method are required. Consequently, climate field reconstructions for the past millennium have focused mainly on regions for which abundant multi-proxy records are available, including Europe (Luterbacher et al., 2004), Northern America (Cook et al., 2004) and East Asia (Shi et al., 2015a). The primary types of proxy records are often tree-ring records and historical documents, mainly because of the data availability and their accurate dating, annual resolution, and demonstrable relationships with instrumental climate data (Fritts, 1976;Zhang, 1991). Other proxy records (e.g., ice core, coral, and varve sediment) have also been introduced into regional climate field reconstructions (e.g., (Neukom et al., 2011)), but they generally represent a small percentage of the data available in global compilations (e.g. (PAGES-2k-Consortium, 2013))~~) but they are generally harder to use~~.

The reconstruction targets ~~for reconstructions~~ are ~~primarily~~ first ~~on~~ temperature ~~variables~~ or temperature-related variables ~~related to temperature because of their large spatial coherency~~. Reconstructions of the localized precipitation field or other variables related to precipitation are seldom (Cook et al., 1999;Casty et al., 2005;Neukom et al., 2013;Cook et al., 2015a;Seftigen et al., 2015) because they require more dense proxy network that it would be the case for temperature ~~they require proxy records with more extensive distributions~~. In particular, the Palmer Drought Severity Index (PDSI) Atlases over the past millennium in North America (North American Drought Atlas, NADA; (Cook et al., 1999)), in Asia (Monsoon Asia Drought Atlas, MADA; (Cook et al., 2010)), in Europe (Old World Drought Atlas, OWDA; (Cook et al.,

2015b)), and in Oceania (Australia and New Zealand summer drought atlas, ANZDA; (Palmer et al., 2015)) were reconstructed using the tree-ring records. All datasets are available at the website of National Oceanic and Atmospheric Administration (NOAA) (~~https://www.ncdc.noaa.gov/cdo/f?p=535:12:0::::P12_rec_id:179~~https://www.ncdc.noaa.gov/data-access/paleoclimatology-data/datasets/climate-reconstruction) and were widely used to identify the variability of droughts and pluvials over the past millennium (e.g., (Cook et al., 2015a)).

The paleoclimate reconstruction methods are divided into climate index reconstruction (CIR) method and climate field reconstruction (CFR) method according to the reconstruction target. The CIRs are mainly derived from two classes of method, direct regression and indirect regression (Christiansen and Ljungqvist, 2017). Methods using the climate variables as the predictands (or dependent variable) and the proxies as the predictors (or independent variable) are called direct regression. On the contrary, the climate variables as the predictors and the proxies as the predictands leads to indirect regression. The composite plus scale (CPS) method is a widely used, classic direct regression, which composites a group of proxy records using uniform or proxy-dependent weighting. The time series obtained is then scaled to have the same variance as the targeted regional or hemispheric averaged variable over a chosen interval. More generally, the regression process is usually based on some forms of univariate or multivariate linear regression and the regression parameters are estimated using classic methods e.g. ordinary least squares, total least squares, variance matching. However, the problem is generally ill-posed because of the limited number of samples in the calibration period and regularized methods have to be introduced, e.g. truncated principal component regression (truncated-PCR) (Mann et al., 1999), Regularized Expectation Maximization (RegEM) (Mann et al., 2008), and Least Absolute Shrinkage and Selection Operator (LASSO) (McShane and Wyner, 2011).

The local (LOC) method is a promising method based on indirect regression. In the LOC method, each proxy record should be first calibrated using the local instrumental climate data, and the time series are then averaged to obtain the large-scale mean climate index (Christiansen, 2011). An indirect regression is used for the local calibration, justified by the fact that the proxy records are functions of climate variables and not the opposite. The reconstructions based on the LOC method are assumed to better preserve the low-frequency climate signal compared to other methods, though they would overestimate the high-frequency signal (Christiansen and Ljungqvist, 2011). Then, the optimal information extraction (OIE) method was proposed to address this bias using the arithmetic mean of the regression coefficients

of the linear regression and the inverse regression (Shi et al., 2012). The hypothesis in the OIE method is that the regression coefficients are random variables with normal distribution that vary in the ranges between the classic linear regression and inverse regression. Additional methods have also been proposed recently to take into account some of the biases of classical methods based on regression such as the pairwise comparison (Hanhijärvi et al., 2013) or Bayesian method of various levels of complexity (e.g.(Tingley and Huybers, 2010)).

The CFR methods can be divided into the reduced space objective analysis-based method (Evans et al., 2000) and the point-to-point regression-based (PPR-based) method (Cook et al., 1999). A typical example of the first group of method is provided by the study of Mann et al. (2009) in which the time coefficients of dominant EOF patterns, calculated from instrumental climate data, are estimated over the pre-instrumental data using a network of proxy records, and then, the climate field over the pre-instrumental data is attained from the product of the reconstructed time coefficients and the instrumental dominant EOF patterns. The underlying hypothesis is that the primary spatial modes of climate change during the instrumental period also explain a large fraction –of the variability in the past. The advantage of this assumption is that only a few proxy records with sparse spatial coverage can be enough to reconstruct a climate field (Neukom et al., 2011). However, the discarded EOF patterns after EOF-truncation may retain some small-scale spatial information, which would have been lost. For instance, the global temperature field reconstruction (Mann et al., 2009) was not consistent with a regional temperature field reconstruction in western Qinling Mountains, China (Yang et al., 2013b). In addition, this method is not well adapted for reconstructions of precipitation field because of the high spatial heterogeneity of this variable (Gómez-Navarro et al., 2015).

The PPR-based method reconstructs each grid point using a linear regression; e.g., PCR (Cook et al., 1999), RegEM regression (Shi et al., 2015a) or the OIE method (Yang et al., 2016) through searching candidate proxy records near the target. The goal of the PPR-based method is to

The climate field reconstruction method can be divided into the Empirical Orthogonal Function-based (EOF-based) method (Mann et al., 2009) and the point-to-point regression-based (PPR-based) method (Cook et al., 1999). The core function of the EOF-based method is to reconstruct the time coefficients of several primary EOF patterns derived from instrumental data. The left EOF patterns may retain some useful regional spatial information, which would have been partially lost in the EOF-based method. For instance, the global temperature field reconstruction using the EOF-based method (Mann et al., 2009)

4

was not consistent with a regional temperature field reconstruction in western Qinling Mountains, China (Yang et al., 2013b). Moreover, the underlying hypothesis is that the primary spatial modes of climate change during the instrumental period also existed in the past and that the order of these principal components have not changed too much with time. The advantage of this assumption is that only a few proxy records with sparse spatial coverage are needed to reconstruct the high-resolution climate field. This approach is generally successful for temperature fields with good spatial correlation (Mann et al., 2009; Neukom et al., 2011) but is more problematic for precipitation fields because of their highly heterogeneous variability (Gómez Navarro et al., 2015).

The PPR-based method reconstructs the climate field for individual grid points with different transform functions; e.g., the Principal Component Regression (PCR) (Cook et al., 1999), the Regularized Expectation Maximization (RegEM) regression (Shi et al., 2015a) and the optimal information extraction (OIE) method (Yang et al., 2016). In theory, the PPR based method maximizes the retention of spatial information, but this method requires a sufficient number of suitable proxy records near the objective grid points.

The precipitation (or the variable sensitive to precipitation) field reconstruction for a large-scale region using the PPR based method is difficult when oSelecting only one type of proxy records, with the associated limited spatial distribution, hinders the field reconstruction of precipitation (or of a variable sensitive to precipitation) for a large-scale region using the PPR-based method. did not cover all reconstruction areas For example, the tree-ring based reconstruction of the MADA provides significant insights into past drought patterns in eastern Asia (Cook et al., 2010), but it performs poorly in reproducing dryness and wetness in eastern China because it only incorporates data from one short tree-ring width chronology from eastern China; . consequentlyConsequently, it would be invalid to extrapolate objective gridded drought variability on the basis of remote tree-ring records in western China (Yang et al., 2013a). Thus, one method to fully consider regional patterns of precipitation is to use the PPR-based method in conjunction with multi-proxy records with good spatial coverage.

Among those PPR based methods, one based on the OIE method (version 1.2) has been successfully applied recently to reconstruct the precipitation field in western Qinling Mountains, China from a multi-proxy dataset (Yang et al., 2016). This OIE method included the ensemble LOC regression (Shi et al., 2012), which was inspired from the original LOC method (Christiansen, 2011). The idea behind the ensemble LOC regression method is that the regression coefficient and error terms are random variables

5

~~with normal distributions within the ranges of the linear regression and inverse regression. The LOC regression method has already been verified to efficiently retain low frequency climate signals (Christiansen, 2011; Shi et al., 2012).~~

In eastern China, there are abundant historical records of precipitation variability (e.g., (Zhang et al., 2003b;Zheng et al., 2006;Hao et al., 2015)). Recently, numerous tree-ring records in western China and surrounding regions have been archived in published databases (Yang et al., 2014b;PAGES2k-Consortium, 2017). This presents an excellent and timely opportunity to integrate the data from tree-ring records from western China and historical records in eastern China to reconstruct the precipitation field for the whole of China. Indeed, Feng et al. (2013) reconstructed the precipitation field in East Asia using composites of multi-proxy records, which are widely used to reflect the variability in precipitation (e.g., Liu et al. (2016)). However, the distribution of proxy records in western China was not sufficiently dense in that reconstruction. In addition, spatial information may have been partially lost using the EOF-based method mentioned above. This is a limitation for developing a further understanding of the dominant patterns of precipitation for the period before instrumental records and their possible driving mechanisms. In this paper, we incorporated additional tree-ring records from western China compared to previous studies and used the PPR-based framework with the OIE method to reconstruct the precipitation field for China. We present an empirical attempt to explore the dominant patterns of precipitation variability before the instrumental period and try to analyse their possible origin.

2 Data and methods

To reconstruct the precipitation field, we used a gridded instrumental precipitation dataset, ~~sensitive precipitation~~ proxy records that can be significantly related to precipitation in the domain studied, and the OIE precipitation field reconstruction method. Other datasets were used to validate the reconstruction and explore possible driving mechanisms.

2.1 Instrumental data

Owing to the highly heterogeneous and localized variability in precipitation, the accuracy of regional precipitation estimates depends mainly on the spatial density of the stations (Wan et al., 2013). Thus, a dense distribution of datasets is considered a priority.

We selected a monthly gridded precipitation dataset, China's Ground Precipitation 0.5° longitude by 0.5° latitude Grid Dataset V2.0 (Zhao and Zhu, 2015), covering the period AD 1961–2010, since this dataset is calculated based on nearly all available national surface stations (n = ~~2474~~2472) in China. We targeted precipitation data from the warm season (May−September, MJJAS) because historical documents mainly record variations in MJJAS precipitation. The whole of China includes 4189 grid points. The calibration period was set to AD 1961~~1981~~ 1990~~2000~~ and the validation period was AD 1991~~1961 1980~~2000. Another instrumental precipitation dataset was used in this study to validate the reconstruction: The Homogenized Monthly Precipitation Dataset in China for the interval 1900–2009 (Li et al., 2012), with a 5° longitude by 5° latitude grid resolution. This dataset includes data from all available national surface stations in China before AD 1960. The MJJAS mean precipitation anomaly for China for the interval AD 1920–1960 is selected here as an independent verification data. Some unusual values were evident for the period before AD 1920, as shown in original Fig.~~ure~~ 12 of Li et al. (2012), and these are likely a result of the sparse distribution of observation points. The two datasets are both developed by, and available from, the National Meteorological Information Center, Chinese Meteorological Administration.

2.2 Tree-ring record

The use of tree-ring records has multiple advantages, including their annual resolution, easy replication, wide distribution, and significant corroboration from instrumental records. Consequently, such records are considered to be primary and practical archives for reconstructing precipitation fields in China over the past half millennium and are widely used to reconstruct regional precipitation variability in China (e.g., (Shao et al., 2005;Yang et al., 2014b)).

The candidate tree-ring records are required to satisfy three~~two~~ conditions: 1) all records must be archived in public repository; 2) each record needs to at least cover the period from AD ~~1876~~1875 to AD ~~1975~~1977; ~~2~~3) if raw tree-ring width measurements are available, they must be based on at least five samples for each year to ensure good replication. The screened 372 chronologies include 371 tree-ring width chronologies and a tree-ring oxygen isotope chronology.

To maximize the overlap lengths of the instrument data and proxy records, all tree-ring records were extrapolated to AD 2000 using the RegEM algorithm (Schneider, 2001). Here, the truncation parameters for the RegEM algorithm were set to the same values as that used by Mann et al. (2008). A total of 197~~242~~ of 372~~491~~ tree-ring chronologies were extrapolated. The maximum and mean extrapolation

lengths of the ~~242~~ 197 chronologies were 23~~24~~ years and ~~10.5~~11 years, respectively. The extrapolation bias was ignored because of the short extrapolation length.

We synthesized 372~~491~~ tree-ring records from China and surrounding area, as shown in ~~Figure~~Fig. 1. The tree-ring records are located mainly in 14 countries including Bhutan, China, India, Japan, Kazakhstan, Kyrgyzstan, Laos, Mongolia, Nepal, Pakistan, Philippines, Russian Federation, Thailand, and Vietnam~~southeastern Asia, the Tibetan Plateau, Xinjiang, Mongolia, and Japan~~. There are only very few tree-ring records in ~~northeastern China and~~ eastern China. This indicates that the currently available tree-ring records are not sufficient for reconstruction of the precipitation field in eastern China.

2.3 Dryness/Wetness index (DWI)

In eastern China, abundant records of drought and flood conditions~~disasters~~ can be found in historical documents, which provide another opportunity to reconstruct past climate (Zhang, 1991;Ge, 2011;Hao et al., 2015). One of the most~~A~~ valuable examples~~~~ is the Yearly Charts of Dryness/Wetness in China for the Last 500-Year Period dataset (Chinese Academy of Meteorological Science, 1981). The DWI dataset, also known as the drought/flood indices (DFI), has been widely used to assess precipitation variability in eastern China (e.g., (Wang and Zhao, 1979;Zhang, 1988;Qian et al., 2003a)). This DWI dataset includes data from 120 locations that are distributed mainly in eastern China and northeastern China, with a few in western China. Herein, ~~12~~13 DWI are excluded because they ~~ir covering~~ too short time periods. The DWI for each year has five grade values: very wet (grade 1), wet (grade 2), normal (grade 3), dry (grade 4), and very dry (grade 5). The DWI dataset is mainly derived from the local chronicles and started from 1470 (the sixth Year of Cheng hua reign in Ming Dynasty), which describe the onset, duration, areal extent, and severity of each drought or flood event in each province, China (Chinese Academy of Meteorological Science, 1981;Zhang, 1983). The experts, mainly from the provincial meteorological bureau provinces, China Meteorological Administration, Peking University, and Chinese Academy of Sciences ~~and so on~~, converted qualitative textual descriptions into quantitative data (Chinese Academy of Meteorological Science, 1981).

The reliability of DWI was described in previous studies (Zhang, 1983;Zhang, 1988). e.g. the homogeneity of DWI was demonstrated using the chi-square test (Zhang, 1983), and the reliability of DWI in spatial pattern was verified through comparison with the eigenvectors of the instrumental precipitation during the period AD 1951-1974 (Wang and Zhao, 1979).

However, DWI have still some weaknesses. The first one is time discontinuity (Zhang, 1983). Figure s1 is the time spans of 107 DWI records. This illustrates that most of DWI records are not continuous in time. The maximum (mean) number of missing values of 107 DWI records during the period AD 1470-2000 was 446 (157). Secondly, the DWI is unevenly distributed over space. Figure s2 shows that the location and number of DWI records during the period AD 1470-2000. On this figure, a value of "100" means that it has 100 observed values during the period AD 1470-2000. It indicates that 91 of 107 DWI records are located in eastern China (east of longitude 105°E), which is the economically developed region. There are only 16 DWI records west of longitude 100°E. Additionally, an uncertainty due to the subjective judgment is unavoidable for the historical documentary, even though the different sources have been used to cross-validate the final reconstruction (Zhang, 1983;Man, 2009;Ge, 2011;Zheng et al., 2014a). Moreover, the range of values is within five grades and the DFI record is not an accurate precipitation value, thus it also limits the accuracy and ability to detect the extreme events (Zheng et al., 2014a).

In order to improve the quality of the DWI dataset, Professor Zhang De'er lead a team of scientists, and carry that carried out a research of during 20 years to identify the weather events in China over the past 3000 years, . This resulted in the publication of a book, entitled "A compendium of Chinese meteorological records of the last 3,000 years". Each record has been carefully cross-checked from more than 8,000 historical documents (Zhang, 2004). However, the updated dataset is not archived in publish repository so far.

This publicly available DWI dataset has been extended to AD 2000 using the annual average and standard deviation of observed rainy season precipitation (May–September, MJJAS) when the instrumental precipitation is available after AD 1980 (Zhang and Liu, 1993;Zhang et al., 2003a). Herein Thus, it does not need to be extrapolated to AD 2000. However, 51 85 DWI records needs to be interpolated because of missing values. The RegEM method was also used to interpolate the DWI data based on their mutual covariance their mutual covariance with the other available data. The maximum (mean) length for interpolation was 400 446 (79157) years. Any interpolation bias was ignored, as the historical documentary data record a regional drought or flood event, rather than a local phenomenon, and they show good regional spatial consistency.

In total, we assembled 600 479 proxy records, which included 489 371 tree-ring width chronologies, 2 a 1 tree-ring oxygen isotope chronologies, and 108 107 DWI, and an instrumental precipitation records from

9

~~South Korea covering AD 1771–2000~~. Each record is required to be significantly correlated with one or more instrumental precipitation record at the 90% (p < 0.1) confidence level during the overlap period, based on both raw data and linearly detrended data. Moreover, previous studies have repeatedly verified a significant relationship between tree-ring precipitation reconstructions and the DWI on a regional scale (e.g.,(Zhang, 2010)). The common period to all of the proxy records is AD 1875–~~1978~~1977. The number of proxy records has a visible changing point from AD 1470 to AD 1469 after extrapolation/interpolation, with a ~~9.50~~41.91% decrease from ~~155~~136 to ~~79~~98. The details for each record are provided in Table s1 and ~~Figure~~Fig. 1.

The two dominant modes of natural climate variability, the El Niño–Southern Oscillation (ENSO) and Pacific Decadal Oscillation (PDO), are used to explore the possible connection between our reconstruction and large-scale variability, since the two indices have already been shown to affect precipitation in China on interannual, interdecadal, and multidecadal timescales based on instrumental analysis (Huang and Wu, 1989;Ma, 2007;Qian and Zhou, 2014)~~)~~. Multiple ENSO and PDO reconstructions over the past millennium have been asse~~ssed~~mbled in our previous work (Shi et al., 2016a). Without loss of generality, we selected three reconstructed ENSO indices (Cook et al., 2008;McGregor et al., 2010;Li et al., 2013a) and three PDO indices (D'Arrigo et al., 2001;D'Arrigo and Wilson, 2006;Shen et al., 2006) that have good performances in relationship with instrumental data. Note that three ENSO indices have a strong significant relationship during the common period AD 1650-1977 with the range of correlation coefficients [0.58, 0.66, 0.84], but the three PDO indices are only very weakly related during their common period AD 1700-1979 with the range of correlation coefficients [0.03, 0.09, 0.13]. As argued recently (e.g. (Newman et al., 2016)), the PDO cannot be considered as a single dynamical process but results of the combined influence of remote tropical forcing and local North Pacific atmosphere–ocean interactions. This makes it a particularly challenging target for proxy-based reconstructions, explaining the poor agreement between the available series.

2.4 Climate model simulation

Six coupled climate models were used to assess whether their past1000 modeling experiments for the interval AD 850–1849 are consistent with our reconstruction. These are BCC-CSM1.1 (Wu et al., 2010b), CCSM4 (Landrum et al., 2012), FGOALS-s2 (Man et al., 2014), GISS-E2-R (Schmidt et al., 2014), IPSL-CM5A-LR (Dufresne et al., 2013), and MPI-ESM-P (Jungclaus et al., 2010). The description of

the six models, sponsoring institutions and main references was shown in Table s3 of Shi et al. (2015a). For details and data of the past1000 experiments, see the websites of the Paleo Modelling Intercomparison Project Phase 3 (PMIP3) and the fifth phase of the Coupled Model Intercomparison Project (CMIP5). All simulated results were interpolated to the same temporal and spatial resolution as the reconstruction in this study.

2.5 Reconstruction method

The OIE method has been successfully used to reconstruct the South Asian summer monsoon index over the past millennium (Shi et al., 2014), the Northern Hemispheric temperature over the past two millennia (Shi et al., 2015b), and the precipitation field over the past 500 years in western Qinling Mountains, China (Yang et al., 2016). The drawback of this method is an overfitting tendency. An independent test data is needed for cross validation to avoid it.

This method (version 1.3~~2~~) within the PPR-based framework comprises three steps. The first step is to search for the candidate proxy records. We firstly selected all possible predictors with significant relation to the target. ~~And t~~Then, we sorted them as a function of ~~in~~ their descending distances from the predictor to the target. We excluded the predictors with distances more than 3500 km. We indeed assumed that the predictor is unlikely to provide useful information about the precipitation variability at the grid point beyond 3500 km. The candidate predictors faced on four possible situations. 1) The number of candidate predictors was more than five, and the first~~ly~~ five predictors included at least one record that could reach AD 1470. This target was constructed using the first~~ly~~ five predictors. Five is the initial minimum number of candidate predictors according to the past experience (Cook et al., 2013). 2) The number of candidate predictors was more than five, but the first~~ly~~ five predictors did not include any record that could reach AD 1470. We increased the number of predictors until a predictor could reach to AD 1470. The target was constructed using the selected predictors, whose number was more than five. 3) The number of candidate predictors is more than five, but no one can reach to AD 1470. We increased the number of predictors until a predictor with the maximum time span. 4) The number of candidate predictors is less than five but more than three. It means that this target cannot meet the requirement of replication, but we tolerate it and use all possible predictors to reconstruct it.

~~We used the search radius method to select those following standard applications of the PPR method~~ ~~(Cook et al., 1999). The search radius is initially set at 450 km according to the precipitation decay~~

correlation distance (New et al., 2000). Five is the minimum number of candidate predictors to ensure good replication of the reconstruction (Cook et al., 2013). If the number of candidate predictors is less than 5, the search radius is extended by 50 km at a time until 5 candidate predictors is found. The maximum search radius is fixed at 3500 km. The second step is to determine the weighting for the proxy record using the correlation coefficient between the candidate proxy record and the reconstructed target according to Shi et al. (2014)'s method. The third step is regression of the proxy record using the ensemble LOC regression method (Shi et al., 2012).

Traditional accuracy and skill parameters, including the square of the Pearson product–moment correlation coefficientexplained variance (r^2) between the reconstruction and the instrumental data during the verification period, the reduction of error (RE) in the verification period, and the coefficient of efficiency (CE) in the verification period (Cook et al., 2010), were used to evaluate the reliability of the reconstructions, and the uncertainty was calculated characterized using the standard deviation of the instrumental precipitation anomaly and the correlation coefficient between the reconstructed and instrumental precipitation anomaly (Mann et al., 2008)residual between the reconstructed and instrumental precipitation data during the verification period.. The significance of the correlation for the filtered time series was accessed using the effective number of degrees of freedom following Zhao et al. (2016) .

The ensemble empirical mode decomposition (EEMD) method (Huang and Wu, 2008;Wu and Huang, 2009) was used to analyse the reconstructed mean MJJAS precipitation time series for eastern China, western China, and the whole of China. The eastern and western China is simply divided along - the longitude 105°. Following Mann et al. (1995), the interannual timescale was set to < 8 years. The interdecadal timescale was defined as ≥8 years and <35 years. The multidecadal timescale was defined as ≥35 years and <100 years, and the centennial scale was >100 years.

The superposed epoch analysis (SEA) is traditionally used to analyse the influence of volcanic eruption on the climate, e.g. Bradley (1988). Here, the code to compute SEA has been downloaded from the website (http://blarquez.com/superposed-epoch-analysis-sea/). The period analysed (time window) are set as 20 years before and after each volcanic eruption event. The 90% confidence limit is estimated using the bootstrap procedure (Blarquez and Carcaillet, 2010). The eruption time series of Sigl et al. (2015) is used here because of the dating improvement compared to earlier estimates. Four categories of volcanic eruption events during the period from AD 1490 to AD 1829 are chosen following Zhuo et al.

(2014)'s method which is based on the magnitude of their sulfate deposition in the Greenland ice-core records: (1) all Northern hemisphere eruption events (CNH0P) according to Sigl et al. (2015), (2) CNH1/2P: the eruption events that have more than half, (3) equal (CNH1P), and (4) double (CNH2P) that of the sulfate deposition of the 1991 Mount Pinatubo eruption.

3 Results and discussion

The quality and reliability of the reconstruction are illustrated in Figures 2−4. Firstly, tThe spatial distribution of the number of predictors for each grid points as a function of the number of predictors is shown in FigureFig. 2a. As mentioned above, the initial minimum number of predictors is five. The 25991737 grids with five candidate proxy records account for 41.562.04% of the grids. The 3760368 grids with ≤10 candidate proxy records account for 80.489.76% of the grids. The maximum number of predictors is 3833. Only seven grids cannot be satisfied with the initial minimum number of predictors (five). This indicates that 99.86% grids have good replication of the reconstruction. In order to reconstruct these seven grids, we tolerate the four grids with four predictors, and the three grids with three predictors. This means that these seven grids were not followed the requirement of the replication.all grid points have enough predictors. Secondly, tThe maximum distance from the predictor to the targetnumber forof each grids for different search radius is shown in FigureFig. 2b. The 15991962 grids with a ≤450-km search radius account for 46.838.17% of the grids. The 34673417 grids with search radii of ≤15000 km account for 81.682.76% of the grids. The maximum distance to the targetsearch radius is 3495.53450 km. This implies that precipitation in most of the grid points can be reconstructed using nearby proxy records.

Thirdly, Figure 3 presents a summary of the reconstruction skills. Figures 3a−, 3b and 3c show that the similarity in the patterns among the r^2, the RE and the CE maps, characterized by a better quality of the reconstruction in eastern China (with the exception of some regions in northeastern China) than in western China. The maximum explained variance is 0.961. The number of grids for which both the RE and CE values are greater than zero is 36313971, accounting for 86.6894.8% of the grids. This indicates that most of the grid points pass the cross-validation process. The uncertainties associated with the grids in southeastern China are greater than those for the grids in northwestern China in Fig. 3d because of large precipitation anomalies in southeastern China.

Finally, Figure 4a compares the reconstructed MJJAS mean precipitation anomalies with the instrumental MJJAS mean precipitation anomalies (Zhao and Zhu, 2015) for China for the interval AD 1961-2000. The reconstructed MJJAS mean precipitation anomalies mostly agree with the instrumental data. The correlation coefficient is 0.89~~1~~ (n = 40), which is significant at the 99% confidence level. Figure 4b compares the reconstructed MJJAS mean precipitation anomalies with the instrumental MJJAS mean precipitation anomalies (Li et al., 2012) in China during AD 1900-2000. The reconstructed MJJAS mean precipitation anomaly is significantly correlated to the instrumental independent data during the interval AD 1920-1960, with a correlation coefficient of 0.59~~7~~ (n = 41), also significant at the 99% confidence level. This indicates that the reconstruction passes the out-of-sample validation on the mean MJJAS precipitation anomalies for China. A part of the disagreements before AD 1919 can come actually from the uncertainties of Li et al. (2012), as ~~specially~~ explained in the instrumental data section.

The evolution of regional mean precipitation anomalies is exhibited in Fig. 5. The different components of the MJJAS precipitation anomalies for eastern China (east of 105°E), western China (west of 105°E), and whole China over the past ~~521~~ 531 years (AD ~~1475~~1470-~~1995~~2000) are obtained using the EEMD method (Fig. 5 and Fig. ~~s1~~s4). The amplitudes of interannual and interdecadal components in eastern China are much larger than in western China (Fig. ~~s1~~s4), but the differences of the amplitudes of other components between eastern and western China are less clear in Fig. 5. The drought/flood changes in eastern and western China are generally consistent over the multidecadal time scale in Fig.5a.

The centennial components in eastern and western China describe both a relative wet climate during the 16th century and a drought during the 17th century. The 17th century drought is also reported in previous studies (e.g., (Wang et al., 2002)). The correlation coefficient of the centennial component in eastern and western China during the interval AD 1470-1749 is 0.87, but the correlation coefficient during the interval AD 1750-2000 is -0.62. Moreover, the 101-year running correlation between the centennial components in eastern and western China shows that a strong significant positive relationship gradually changed to a weak significant negative relationship during the late 18th century (figure not shown). This may suggest that the driver of the centennial component has changed after the late of 18th century.

~~There is an opposite sign , but~~ ~~in the~~ The long-term trends in eastern and western China have opposite signs ~~have opposite signs~~. The long-term trend in eastern China can be broadly divided into two~~three~~ periods: during the first phase before the early 18th ~~17th~~ century there was a wetting trend~~is a partial~~ ~~drought condition, the second stage is wet condition from the early 17th century to the early 20th century~~,

14

and then, the ~~secondthird stage gradually becomes a significant drought~~ condition~~s~~ become dryer until now, which is consistent in previous studies (e.g., (Zheng et al., 2006;Pei et al., 2015)). The long-term trend in western China can also be divided two stages~~,~~: during the first stage from the late 15th century to the late 16th ~~early 19th~~ century there was~~is~~ a ~~drought~~ drying trend~~condition~~, and then, the~~n~~ second stage ~~gradually become a significant~~corresponds to gradually wet~~ter~~ condition~~s~~ until now. The long-term trend for whole China has similarities with the one in eastern China, but with a much weaker amplitude. ~~The centennial components in eastern and western China describe both a relative wet climate during the 16th century and a drought during the 17th century. The 17th century drought is also reported in previous studies (e.g., (Wang et al., 2002)). Moreover, the correlation coefficient of the centennial component in eastern and western China during the interval AD 1475-1849 is 0.67, but the correlation coefficient during the interval AD 1849-1995 is -0.39. This may suggest that the driver of the centennial component has changed after AD 1849.~~

Figure 6 shows the spatial patterns of the May–September precipitation field relative to the 1961–90 climatological mean during five severe droughts in China. The selection of five drought periods follows Feng et al. (2013)~~,~~ but the spatial patterns in our reconstruction display some clear differences from their results . A "north drought with south flooding" dipole pattern in eastern China is seen in Figures 6a−d, and there is a triple pattern in eastern China in Fig. 6e. A similar dipole pattern can be found in Figures 5b and 5d (Feng et al., 2013) for two drought events (AD 1586−89 and AD 1876−78) but during four out of five drought periods, most of northeastern China is relatively humid situation in our study, which is not consistent with Feng et al. (2013)'s Fig. 5. An exceptional drought condition in northeastern China appears in the 1876-1878 drought event, which is the most severe drought of five events in eastern China. We have also calculated the spatial correlation between Cook's MADA PDSI reconstruction (Cook et al., 2010) with our precipitation reconstruction in Fig. s3. Strong correlations appear in the northeastern Tibetan Plateau, where there are longest and most abundant tree-ring width chronologies in China. Here, the precipitation is possibly a primary control factor of the tree-ring width chronology (Zhang et al., 2003c;Yang et al., 2014b). There are weak correlations between the reconstructions in eastern China even through the correlation coefficients are significant in some regions. The MADA is not consistent with the DWI records in eastern China, since only very few and short tree-ring width chronologies in eastern China are used to reconstruct the MADA (Yang et al., 2013a;Kang et al., 2014;Yang et al., 2014a;Zheng et al., 2014b;Ge et al., 2016).

15

We compared the precipitation reconstruction with the six climate model simulations in Figures 7−8. We start our analysis in AD 1470 since, before that date, there are no available historical document and the quality of the reconstruction is thus likely low. The analysis of spatial pattern covers the period AD 1470-1849 as we specifically focus on the pre-industrial period. The more recent past has been the subject of some recent studies and different factors such as the changes in aerosol concentration may have a dominant effect then (Li et al., 2016).

We focus on the period during AD 1470-1849, which is a compromise between the common period of the past1000 climate model experiments (AD 850–1849) and the plausible reconstruction (AD 1470–2000). We only use the reconstruction after AD 1470 since there are no historical documents before that date. The reference period is AD 1961-1990. Figure 76 shows the reconstructed 9-year running mean MJJAS precipitation anomalies for China for the interval AD 1470–2000 compared with six climate model simulations.

Only the CCSM4FGOALS-s2 results are significantly correlated with the reconstructed results during AD 1470–1849 at the 95% confidence level, but the correlation is low negative (r = -0.160.23). Furthermore, there is distinct shift between the mean values of the CCSM4FGOALS-s2 results and the reconstruction over that period. This is related to the choice of the reference period and the increasing trend in FGOALS-s2 model since the mid-19th century in the reconstruction. All climate model simulations show low correlations with the reconstructed result. The correlation of the simulated times series is also weak between the different models. This suggests that MJJAS mean precipitation anomalies over the past 380 years in China may be largely controlled by the internal variability rather than by external forcing during the interval (AD 1470–1849). Similar conclusions were derived from the comparison of reconstructed and simulated hydroclimatic variables over the past millennium in North America (Coats et al., 2015) and in East Africa (Klein et al., 2016).

Traditional EOF analysis was applied to reveal the spatial patterns in MJJAS precipitation anomalies in China over a 380-year interval (AD 1470–1849). The first four EOFs are well separated according to North et al. (1982) criteria, but the fourth EOFs only accounts for 5.14.7% of total variance, and its pattern is unusual in compared to previous studies. Thus, the first three EOF patterns and their corresponding time coefficients (also known as principal components, PCs) of the reconstructed MJJAS precipitation fields in China are compared with six climate model simulations in FigureFig. 78.

The first EOF leading mode of the ~~reconstructed~~ MJJAS precipitation field (Fig. ~~7a~~8a) displays a main loading in eastern China, and a general (monopole) variation over most of China, with the exception of the northeastern and western margins of the Tibetan Plateau. This mode accounts for ~~19.0~~16.6% of the total variance, which is lower than the leading mode of temperature field (Shi et al., 2015a), but it is normal in precipitation analysis (Day et al., 2015). A main loading in eastern China also appears in the EOF1 of the reconstructed MJJAS precipitation anomalies during the interval (AD 1850–2000), the EOF1 of the reconstructed data during the interval (AD 1961–2000) and the EOF1 of the instrumental data during the same interval (AD 1961–2000). A main loading of EOF1 in eastern China is also consistent with other previous results (Wang and Zhao, 1979;Qian et al., 2003a). This is due to the large variance in eastern China, which causes the larger loads in eastern China in the other two EOFs. The EOF1 of IPSL-CM5A-LR, the EOF2 of MPI-ESM-P, and the EOF3 of CCSM4 also show a consistent variation in most of eastern China, but also some differences with the pattern deduced from the reconstruction. Furthermore. the corresponding time coefficients of model EOFs shows no obvious significant relationship with the reconstructed data (figure not shown), which was expected if natural variability is the main driver of the changes.

The second leading mode of the MJJAS precipitation field (Fig. ~~7b~~8b) demonstrates a south–north anomalous rainfall dipole pattern, with drying in the middle and lower reaches of the Yellow River, and increasing rainfall across and to the south of the Yangtze River. This mode accounts for ~~12.6~~11.2% of the total variance and also appears in the EOF2 of the reconstructed MJJAS precipitation anomalies during the interval (AD 1850–2000). The South-Flood North-Drought pattern is commonly referred in previous studies from an analysis of DWI (e.g., (Wang and Zhao, 1979;Qian et al., 2003a) and instrumental data (e.g., , (Huang et al., 1999;Yu and Zhou, 2007;Ding et al., 2008;Zhou et al., 2009). Moreover, the variations have the same sign in most of western China and northern~~southeastern~~ China, except for Xinjiang province. The EOF1 from three climate models (CCSM4, FGOALS-s2, GISS-E2-R), the EOF2 from BCC-CSM1.1 model, and the EOF3 from MPI-ESM-P model reproduce a similar south–north dipole pattern in eastern China to the reconstructed results, but the specific range for each model is different. Moreover, their corresponding time coefficients show that no climate model simulation demonstrates a significant relationship with the reconstructed result (figure not shown). As mentioned for EOF1, this may be perfectly well justified if the variability of the south–north dipole pattern is dominated by internal variability.

The third leading mode illustrates a "sandwich" triple precipitation pattern with increasing rainfall in the area covering the middle and lower reaches of the Yangtze River valley, drying over southern and northern China, and variations of the same sign in most of western China and central China (Fig. 7e8c). This mode accounts for 8.17.9% of the total variance. The "sandwich" triple mode in eastern China has been reported based on the analysis of DWI (e.g., (Wang and Zhao, 1979;Qian et al., 2003b)) and instrumental data (e.g., (Ding et al., 2008)). The EOF1 from two climate models (BCC-CSM1.1 and MPI-ESM-P), the EOF2 from CCSM4 model, the EOF3 from IPSL-CM5A-LR model show similar "sandwich" triple mode to the reconstruction, and their corresponding time coefficients have again no significant relationship with the reconstructed result at the 90% confidence level (figure not shown).

4 Discussion

In order to explore the origins of three dominant modes, wThe first dominant mode of precipitation field with annual resolution is characterized by a monopole over all China, with the largest loading in eastern China indicating a co-variability of precipitation between monsoon and non-monsoon regions. We firstly consider the influence of the external forcing on the MJJAS precipitation anomalies variability during AD 1470-1849. The impact of the Northern Hemisphere volcanic eruptions on the precipitation field for the four categories of eruption (CNH0P, CNH1/2P, CNH1P, and CNH2P) is shown in Fig. s5. The superposed epoch analysis (SEA) results applied to between the mean precipitation anomalies (Fig. s5a), and its PC1 (Fig. s5b), and 35 large eruption events during AD 14970-18249 shows that volcanic activity as one important external forcing may might affect the MJJAS precipitation anomalies variability for China (Fig. 8). Nevertheless, the signals are barely significant and there are similar averaged scores before and after the volcanic eruption year. Moreover, the spatial patterns of the impact of the Northern Hemisphere volcanic eruption events on the precipitation field (Figures s5c−f) is not consistent between the four categories of eruption (CNH0P, CNH1/2P, CNH1P, and CNH2P), suggesting a weak influence of the eruption. . This indicates that the response of MJJAS precipitation anomalies for China to Northern Hemispheric volcanic eruption is not robust.

The solar activity, as another potentially important external forcing, may also be part of the driving mechanism. This view is supported by the fact that the PC1 shows a weak significant relationship with solar activity index (Wang et al., 2005) (r = 0.1719, n = 239240) at the 95% confidence level for the interval AD 16104–1849. The correlation coefficient reaches 0.33 35 after the 11-year running mean filter. In summary, the influences of volcanic eruption and solar activity on PC1 are not very strong in

our results. A pattern showing some similarities to the PC1 of the reconstructions appears in three climate models (Fig. 78a), but the differences, in particular in western China, are too large to ensure that it has the same dynamical origin and to use model results to determine the origin of the reconstructed pattern.

The second mode of annual precipitation field is the north–south dipole mode in eastern China, with variations of the same sign in most of western China and northernsoutheastern China, except for Xinjiang province. In fact, the north-south dipole pattern of the precipitation in eastern China was found over centennial timescale during the Medieval Warm Period and the Little Ice Age from the historical documents and speleothem records (e.g., (Wang et al., 2001) and was one of dominant modes over interdecadal timescale (e.g., Ding et al., 2008).

In order to explore its possible origin, we have calculated the running correlation between the 17 reconstructed ENSO indices and the precipitation anomalies averaged over Yangtze River region and Huai River region with a window size of 101 years (Figures not shown). The correlation varied between negative and positive values, but there was small positive and significant correlation, when we have calculated the correlation coefficient for the full period. This indicates that the relationship between ENSO and summer precipitation in China is not stable in time, which is consistent with the instrumental period (Wu and Wang, 2002). However, if we analyse the full period, a more robust link between ENSO and summer precipitation in China may be found. w

We calculated the correlation of the precipitation field with the annual mean (over the months July–June) ENSO index of McGregor et al. (2010), as shown in FigureFig. 9. The results show a similar pattern with a north–south dipole mode in eastern China, and the precipitation anomalies in most of western China have a positive correlation with ENSO at the 90% confidence level. In addition, PC2 is significantly correlated with the ENSO index reconstruction (McGregor et al., 2010) at the 99% level (r = 0.3022, n =200) during the interval AD 1650–1849. Moreover, the other two other ENSO indices (Cook et al., 2008;Li et al., 2013a) give similar correlation maps with the precipitation field (Fig. s2s6), but a lower correlation coefficients with PC2. This indicates that the north–south dipole in eastern China and variations of the same sign in most of western China and northernsoutheastern China, except for Xinjiang province, are likely influenced by ENSO variability before the Industrial Revolution in our reconstruction. FurtherlyFinally, wWe calculated simulated Niño 3.4 in different seasons including the annual mean (over the months July–June), previous July to current June, previous December–January–February (DJF), current March–April–May (MAM), current June–July–August (JJA) and current MJJAS seasons. The

correlation maps of five simulated MJJAS mean precipitation anomalies for China with the five-corresponding simulated annual mean Niño 3.4 indices are shown in Fig. 9. They display similar south-north dipole correlation patterns in eastern China, similar to the one from the reconstruction, for three climate models (BCC-CSM1-1, CCSM4, and MPI-ESM-P). The relationship between the previous winter (December–January–February) Niño 3.4 index and the precipitation field for each model is shown in Fig. s7. The spatial pattern is very similar with the result of annual mean Niño 3.4 index. The Niño3.4 indices in previous July to current June, previous December–January–February (DJF) and current March–April–May (MAM) seasons during AD 1470-1849 in CCSM4 model are significantly related to its PC1 at the 99% confidence level, and the correlation coefficients are 0.30, 0.30 and 0.27, respectively. The Niño3.4 indices in current June–July–August (JJA) and MJJAS seasons in FGOALS-s2 model during AD 1470-1849 are significantly related to its PC1 at the 99% confidence level, and the correlation coefficients both are 0.16. The Niño3.4 indices in previous July to current June, previous DJF, current MAM, JJA and MJJAS seasons during AD 1470-1849 in MPI-ESM-P model are significantly related to its PC3 at the 99% confidence level, the correlation coefficients are 0.23, 0.22, 0.20, 0.18, and 0.19, respectively. The EOF1 of CCSM4 model, the EOF1 of FGOALS-s2 model and the EOF3 of MPI-ESM-P model all show a similar south-north dipole mode, even the specific ranges of their spatial patterns are different. This demonstrates that ENSO has likely an imprint on the south-north dipole mode of the precipitation pattern in eastern China during AD 1470-1849 in those simulations.

Those results are consistent with previous studies based on PIMIP3 model simulations suggested that La Niña (El Niño)-like conditions may explain the north-south dipole in eastern China on centennial timescale (e.g., (Shi et al., 2016b) and with instrumental observations indicating that ENSO was associated with summer rainfall in eastern China (e.g., (Huang and Wu, 1989;Guo et al., 2012;Schubert et al., 2016). Based on instrumental data analysis, three general views, are used to explain the precipitation variability in eastern Asia linked to ENSO, and all of them emphasize the important bridge role of the anomalous western North Pacific anticyclone. The first one is the equatorial Rossby wave response to ENSO via the Pacific-East Asia teleconnection(Wang et al., 2000;Zhang et al., 2011;Karori et al., 2013;Feng et al., 2016). The second one is equatorial Kelvin wave response to Indian Ocean warming during El Niño decaying summer which is named "Indian Ocean capacitor effect" (Xie et al., 2009). The more recent third one is the nonlinear atmospheric interactions between ENSO and the annual cycle (Stuecker et al., 2013;Zhang et al., 2016).

We calculated the correlation map of the precipitation field with the PDO index (D'Arrigo et al., 2001) applying a 9–year running mean filter (Fig. s2). The results at the 90% confidence level show a pattern similar to EOF2 with a north–south dipole mode in eastern China. Moreover, the relationship between PDO index (D'Arrigo et al., 2001) and PC2 is strongly significant ($r = 0.41$, $n = 150$) during AD 1700–1849 at 95% confidence level after a 9-year running mean filter. However, the other two PDO indices (D'Arrigo and Wilson, 2006;Shen et al., 2006) give different correlation maps with the precipitation field (Fig. s2), and lower correlation coefficients (-0.2536 and 0.0736) with PC2 after a 9-year running mean filter. This indicates that the EOF2 mode is also possibly related to variations in the PDO, but the result is sensitive to the choice of the reconstructed PDO index.

Based on the instrumental data analysis, the "sandwich" triple mode in eastern China is likely associated with a meridional tripolar teleconnection in eastern Asia: the Pacific-Japan (PJ; (Nitta, 1987)), Pacific-East Asia (EAP, (Huang and Li, 1988)), or Indo-Asia-Pacific (IAP; (Li et al., 2013b)). The PJ/EAP/IAP teleconnection pattern can be considered as an internal mode mainly controlled by atmospheric processes (Hirota and Takahashi, 2012;Zhang and Zhou, 2015). It also can be forced by the external heating such as the anomalous convective activity in the western Pacific and tropical Indian Ocean during the El Niño decaying year (Huang and Li, 1988;Li et al., 2013b;Xie et al., 2009;Wu et al., 2010a). However, there is no district evidence from the correlation maps of the reconstructed precipitation field with the ENSO and PDO indices to support this kind of mechanism for the "sandwich" pattern in this study. Alternatively, a new hypothesis was proposed recently to explain the "sandwich" triple mode through the interannual change in the strength of moisture transport from the Bay of Bengal to the Yangtze corridor across the northern Yunnan Plateau (Day et al., 2015). The increased latent heating associated with an increase in water vapor along the Yangtze corridor may generate the triple mode in eastern China and variations of the same sign in most of western China and central China.

Our results indicate thus that the south-north mode variability of precipitation anomalies in China carries very likely the fingerprint of ENSO evolution in tropical Pacific over the past 500 years. T, but the origin of the EOF1 and EOF3 patterns are is not clearly established yet, even though both of them maybe closely related to the western pacific subtropical high during the instrumental period (Wu and Wang, 2002). Moreover, some studies showThis implies that the other factors such as the North Atlantic Oscillation (NAO)(Wu et al., 2009;Zheng et al., 2016), and the North Atlantic triple SST pattern (Ruan and Li, 2016), the interdecadal Pacific oscillation (IPO) (Song and Zhou, 2015), North Atlantic triple SST pattern (Ruan

21

and Li, 2016) through the North Atlantic–Eurasia Teleconnection (AEAT) (Li et al., 2013a), the snow cover change of the Tibetan Plateau (Ding et al., 2009;Wu et al., 2012) , and changes aerosol concentration (Li et al., 2016) some regional processes in China may contribute to the reconstructed precipitation field modes during the instrumentalpre-industrial period. Thus, additional studies are then required to determine which of these processes might be related to EOF1 and EOF3 over the pre-industrial period.

Some climate models (e.g., CCSM4, MPI-ESM-P) can broadly reproduce some of the dominant spatial patterns of variability of the reconstructed precipitation field for period studied. Nevertheless, the corresponding time coefficients does not match with the reconstructed series. A possible reason for this is that the precipitation changes are controlled by internal variability (e.g. related to ENSO). By constraining model result to follow the observed time series, data assimilation may then provide an interesting opportunity to analyse in more detail the mechanisms at the origin of the reconstructed changes (e.g., (Widmann et al., 2010;Hakim et al., 2016)).

45 Conclusions

The precipitation field for all of China was reconstructed for the past half millennium using the OIE method and additional proxy records compared to previous studies. The reconstruction shows good performance through the cross-validation process and comparison with "out-of-sample" instrumental data.

The precipitation field reconstruction reveals three leading modes for the period AD 1470–1849 before the Industrial Revolution. The first dominant mode shows consistent variation across most of China, with the exception of the northweastern Tibetan Plateau and some areawestern margins of the Xinjiang province Tibetan Plateau. This mode does not appear to be associated to the response to volcanic eruption or the solar activity. A hypothesis is that such homogenous precipitation variations in various climate regions in China have their origin in the internal variability of the system but it was not possible to determine in the present framework through which mechanism. The second mode, comprising a north–south dipole in eastern China and variations of the same sign in most of western China and southeastern northern China, except for Xinjiang province. The correlation with different reconstructions of ENSO

index indicates that this dipole is likely related to variations in ENSO. The third mode is a "sandwich" triple mode in eastern China and variations of the same sign in most of western China and central China. Moreover, the precipitation field reconstruction was used to assess the skill of PMIP3 coupled climate models. For most models, the dominant mode of variability is not characterized by relatively homogenous changes over all China, in contrast to the reconstructed fields. The correlation map between the five simulated MJJAS mean precipitation anomalies for China with the five-corresponding simulated annual mean Niño 3.4 indices shows that the ENSO has likely an imprint on the south-north dipole mode of precipitation anomaly in eastern China over the half past millennium in the simulations too. However, there is a clear model-reconstruction mismatch in reproducing the corresponding time development as they are not able to reproduce the timing of events associated to internal variability.

Data availability: The 479 proxy records include 247 tree-ring width chronologies and a tree-ring $\delta^{18}O$ chronology archived in International Tree Ring Data Bank (ITRDB) (https://www.ncdc.noaa.gov/data-access/paleoclimatology-data/datasets/tree-ring), 77 tree-ring width chronologies in the supplement of the book (Li et al., 2000), 37 tree-ring chronologies in the PAGES2k dataset v2.0 (https://figshare.com/s/d327a0367bb908a4c4f2), 10 tree-ring width chronologies and 107 Dryness/Wetness records at the webpages of the Chinese Meteorological Data Service Center (CMDC) (http://data.cma.cn/data/detail/dataCode/HPXY_HDOC_CHN_DAW.html, and http://data.cma.cn/data/cdcdetail/dataCode/HPXY_TRRI_CHN.html). The two instrumental precipitation datasets are both archived by the Chinese Meteorological Data Service Center (CMDC). The China's Ground Precipitation Dataset V2.0 can be obtained from the website (http://data.cma.cn/data/detail/dataCode/SURF_CLI_CHN_PRE_MON_GRID_0.5.html) and the Homogenized Monthly Precipitation Dataset in China can be downloaded from the website (http://data.cma.cn/data/detail/dataCode/SEVP_CLI_CHN_PRE_MON_GRID.html). We will archive the code for the OIE (version 1.3) method on GitHub website after this work published.

References

Bradley, R. S.: The explosive volcanic eruption signal in Northern Hemisphere continental temperature records, Clim. Change 12, 221-243, 1988.

Casty, C., Wanner, H., Luterbacher, J., Esper, J., and Bohm, R.: Temperature and precipitation variability in the european Alps since 1500, Int. J. Climatol. , 25, 1855-1880, 2005.

Chinese Academy of Meteorological Science, C. M. A.: Yearly charts of dryness/wetness in China for the last 500-year period, Cartological Press, Beijing, China, 1981.

Christiansen, B.: Reconstructing the NH mean temperature: Can underestimation of trends and variability be avoided?, J. Climate, 24, 674-692, doi:10.1175/2010jcli3646.1, 2011.

Christiansen, B., and Ljungqvist, F. C.: Reconstruction of the Extratropical NH Mean Temperature over the Last Millennium with a Method that Preserves Low-Frequency Variability, J. Climate, 24, 6013-6034, doi:10.1175/2011jcli4145.1, 2011.

Christiansen, B., and Ljungqvist, F. C.: Challenges and perspectives for large-scale temperature reconstructions of the past two millennia, Rev. Geophys. , 55, 40-96, doi:10.1002/2016RG000521, 2017.

Coats, S., Smerdon, J. E., Cook, B. I., and Seager, R.: Are simulated megadroughts in the North American southwest forced?, J. Climate, 28, 124-142, 2015.

Cook, B. I., Ault, T. R., and Smerdon, J. E.: Unprecedented 21st century drought risk in the American Southwest and Central Plains, Sci. Adv., 1, doi:10.1126/sciadv.1400082, 2015a.

Cook, E. R., Meko, D. M., Stahle, D. W., and Cleaveland, M. K.: Drought reconstructions for the continental United States, J. Climate, 12, 1145-1162, 1999.

Cook, E. R., Woodhouse, C. A., Eakin, C. M., Meko, D. M., and Stahle, D. W.: Long-term aridity changes in the western United States, Science, 306, 1015-1018, 2004.

Cook, E. R., D'Arrigo, R. D., Anchukaitis, K. J., and Diaz, H. F.: ENSO reconstructions from long tree-ring chronologies: Unifying the differences, Talk presented at a special workshop on Reconciling ENSO Chronologies for the Past, 2008,

Cook, E. R., Anchukaitis, K. J., Buckley, B. M., D'Arrigo, R., Jacoby, G. C., and Wright, W. E.: Asian monsoon failure and megadrought during the last millennium, Science, 328, 486-489, doi:10.1126/science.1185188, 2010.

Cook, E. R., Krusic, P. J., Anchukaitis, K. J., Buckley, B. M., Nakatsuka, T., and Sano, M.: Tree-ring reconstructed summer temperature anomalies for temperate East Asia since 800 CE, Clim. Dyn., 41, 2957-2972, doi:10.1007/s00382-012-1611-x, 2013.

Cook, E. R., Seager, R., Kushnir, Y., Briffa, K. R., Büntgen, U., Frank, D., Krusic, P. J., Tegel, W., van der Schrier, G., Andreu-Hayles, L., Baillie, M., Baittinger, C., Bleicher, N., Bonde, N., Brown, D., Carrer, M., Cooper, R., Čufar, K., Dittmar, C., Esper, J., Griggs, C., Gunnarson, B., Günther, B., Gutierrez, E., Haneca, K., Helama, S., Herzig, F., Heussner, K.-U., Hofmann, J., Janda, P., Kontic, R., Köse, N., Kyncl, T., Levanič, T., Linderholm, H., Manning, S., Melvin, T. M., Miles, D., Neuwirth, B., Nicolussi, K., Nola, P., Panayotov, M., Popa, I., Rothe, A., Seftigen, K., Seim, A., Svarva, H., Svoboda, M., Thun, T.,

Timonen, M., Touchan, R., Trotsiuk, V., Trouet, V., Walder, F., Ważny, T., Wilson, R., and Zang, C.: Old World megadroughts and pluvials during the Common Era, Sci. Adv., 1, doi:10.1126/sciadv.1500561, 2015b.

D'Arrigo, R., Villalba, R., and Wiles, G.: Tree-ring estimates of Pacific decadal climate variability, Clim. Dyn., 18, 219-224, doi:10.1007/s003820100177, 2001.

D'Arrigo, R., and Wilson, R.: On the Asian expression of the PDO, Int. J. Climatol. , 26, 1607-1617, doi:10.1002/joc.1326, 2006.

Day, J. A., Fung, I. Y., and Risi, C.: Coupling of South and East Asian Monsoon Precipitation in July–August, J. Climate, 28, 4330-4356, doi:10.1175/JCLI-D-14-00393.1, 2015.

Ding, Y. H., Wang, Z. Y., and Sun, Y.: Inter-decadal variation of the summer precipitation in East China and its association with decreasing Asian summer monsoon. Part I: Observed evidences, Int. J. Climatol. , 28, 1139-1161, doi:10.1002/joc.1615, 2008.

Ding, Y. H., Sun, Y., Wang, Z. Y., Zhu, Y. X., and Song, Y. F.: Inter-decadal variation of the summer precipitation in China and its association with decreasing Asian summer monsoon Part II: Possible causes, Int. J. Climatol. , 29, 1926-1944, doi:10.1002/joc.1759, 2009.

Dufresne, J.-L., Foujols, M.-A., Denvil, S., Caubel, A., Marti, O., Aumont, O., Balkanski, Y., Bekki, S., Bellenger, H., and Benshila, R.: Climate change projections using the IPSL-CM5 Earth System Model: from CMIP3 to CMIP5, Clim. Dyn., 40, 2123-2165, 2013.

Evans, M., Kaplan, A., Cane, M., and Villalba, R.: Globality and optimality in climate field reconstructions from proxy data, Present and Past Interhemispheric climate linkages in the Americas and their Societal Effects, 53-72, 2000.

Feng, J., Li, J. P., Zheng, F., and Sun, C.: Contrasting impacts of developing phases of two types of El Niño on southern China rainfall, J. Meteor. Soc. Japan, 94, 359-370, 2016.

Feng, S., Hu, Q., Wu, Q., and Mann, M. E.: A gridded reconstruction of warm season precipitation for Asia spanning the past half millennium, J. Climate, 26, 2192-2204, doi:10.1175/jcli-d-12-00099.1, 2013.

Fritts, H.: Tree rings and climate, Academic Press London, 1976.

Ge, Q.: The climate change in China during the past dynasties, Science Press, Beijing, 61-665 pp., 2011.

Ge, Q., Zheng, J., Hao, Z., Liu, Y., and Li, M.: Recent advances on reconstruction of climate and extreme events in China for the past 2000 years, J. Geog. Sci. , 26, 827-854, doi:10.1007/s11442-016-1301-4, 2016.

Gómez-Navarro, J. J., Werner, J., Wagner, S., Luterbacher, J., and Zorita, E.: Establishing the skill of climate field reconstruction techniques for precipitation with pseudoproxy experiments, Clim. Dyn., 45, 1395-1413, doi:10.1007/s00382-014-2388-x, 2015.

Guo, Y., Li, J., and Li, Y.: A time-scale decomposition approach to statistically downscale summer rainfall over North China, J. Climate, 25, 572-591, doi:10.1175/JCLI-D-11-00014.1, 2012.

Hakim, G. J., Emile-Geay, J., Steig, E. J., Noone, D., Anderson, D. M., Tardif, R., Steiger, N., and Perkins, W. A.: The last millennium climate reanalysis project: Framework and first results, J. Geophys. Res. [Atmos.], 121, 6745-6764, 2016.

Hanhijärvi, S., Tingley, M., and Korhola, A.: Pairwise comparisons to reconstruct mean temperature in the Arctic Atlantic Region over the last 2,000 years, Clim. Dyn., 41, 2039-2060, doi:10.1007/s00382-013-1701-4, 2013.

Hirota, N., and Takahashi, M.: A tripolar pattern as an internal mode of the East Asian summer monsoon, Clim. Dyn., 39, 2219-2238, 2012.

Huang, R., and Li, W.: Influence of heat source anomaly over the western tropical Pacific on the subtropical high over East Asia during summer and its physical mechanism, Chin. J. Atmos. Sci., 107-117, 1988.

Huang, R., and Wu, Y.: The influence of ENSO on the summer climate change in China and its mechanism, Adv. Atmos. Sci. , 6, 21-32, 1989.

Huang, R. H., Xu, Y. H., and Zhou, L. T.: The interdecadal variation of summer precipitations in China and the drought trend in North China, Plateau Meteorology, 18, 465-476, 1999.

Jungclaus, J. H., Lorenz, S. J., Timmreck, C., Reick, C. H., Brovkin, V., Six, K., Segschneider, J., Giorgetta, M. A., Crowley, T. J., Pongratz, J., Krivova, N. A., Vieira, L. E., Solanki, S. K., Klocke, D., Botzet, M., Esch, M., Gayler, V., Haak, H., Raddatz, T. J., Roeckner, E., Schnur, R., Widmann, H., Claussen, M., Stevens, B., and Marotzke, J.: Climate and carbon-cycle variability over the last millennium, Clim Past, 6, 723-737, 2010.

Kang, S., Bräuning, A., and Ge, H.: Tree-ring based evidence of the multi-decadal climatic oscillation during the past 200 years in north-central China, Journal of Arid Environments, 110, 53-59, doi:https://doi.org/10.1016/j.jaridenv.2014.06.003, 2014.

Karori, M. A., Li, J., and Jin, F.-F.: The asymmetric influence of the two types of El Niño and La Niña on summer rainfall over Southeast China, J. Climate, 26, 4567-4582, 2013.

Klein, F., Goosse, H., Graham, N. E., and Verschuren, D.: Comparison of simulated and reconstructed variations in East African hydroclimate over the last millennium, Clim Past, 12, 1499-1518, doi:10.5194/cp-12-1499-2016, 2016.

Landrum, L., Otto-Bliesner, B. L., Wahl, E. R., Conley, A., Lawrence, P. J., Rosenbloom, N., and Teng, H.: Last millennium climate and its variability in CCSM4, J. Climate, 26, 1085-1111, doi:10.1175/JCLI-D-11-00326.1, 2012.

Li, J., Xie, S.-P., Cook, E. R., Morales, M. S., Christie, D. A., Johnson, N. C., Chen, F., D'Arrigo, R., Fowler, A. M., Gou, X., and Fang, K.: El Niño modulations over the past seven centuries, Nature Climate Change, 3, 822-826, doi:10.1038/nclimate1936, 2013a.

Li, J. P., Ren, R. C., Qi, Y. Q., Wang, F. M., Lu, R. Y., Zhang, P. Q., Jiang, Z. H., Duan, W. S., Yu, F., and Yang, Y. Z.: Progress in air-land-sea interactions in Asia and their role in global and Asian climate change, Chin. J. Atmos. Sci., 37, 518-538, 2013b.

Li, Q., Peng, J., and Shen, Y.: Development of China homogenized monthly precipitation dataset during 1900-2009, J. Geog. Sci. , 22, 579-593, 2012.

Li, Z., Lau, W. K. M., Ramanathan, V., Wu, G., Ding, Y., Manoj, M. G., Liu, J., Qian, Y., Li, J., Zhou, T., Fan, J., Rosenfeld, D., Ming, Y., Wang, Y., Huang, J., Wang, B., Xu, X., Lee, S. S., Cribb, M., Zhang, F., Yang, X., Zhao, C., Takemura, T., Wang, K., Xia, X., Yin, Y., Zhang, H., Guo, J., Zhai, P. M., Sugimoto, N., Babu, S. S., and Brasseur, G. P.: Aerosol and monsoon climate interactions over Asia, Rev. Geophys. , 54, 866-929, doi:10.1002/2015RG000500, 2016.

Liu, F., Chai, J., Wang, B., Liu, J., Zhang, X., and Wang, Z.: Global monsoon precipitation responses to large volcanic eruptions, Scientific Reports, 6, 24331, doi:10.1038/srep24331, 2016.

Luterbacher, J., Dietrich, D., Xoplaki, E., Grosjean, M., and Wanner, H.: European seasonal and annual temperature variability, trends, and extremes since 1500, Science, 303, 1499-1503, 2004.

Ma, Z.: The interdecadal trend and shift of dry/wet over the central part of North China and their relationship to the Pacific Decadal Oscillation (PDO), Chin. Sci. Bull., 52, 2130-2139, doi:10.1007/s11434-007-0284-z, 2007.

Man, W., Zhou, T., and Jungclaus, J. H.: Effects of large volcanic eruptions on global summer climate and East Asian monsoon changes during the Last millennium: Analysis of MPI-ESM simulations, J. Climate, 27, 7394-7409, doi:10.1175/JCLI-D-13-00739.1, 2014.

Man, Z. M.: Climatic change historical period of China, Shandong Education Press, Jinan, 2009.

Mann, M. E., Park, J., and Bradley, R.: Global interdecadal and century-scale climate oscillations during the past five centuries, Nature, 378, 266-270, doi:10.1038/378266a0, 1995.

Mann, M. E., Bradley, R. S., and Hughes, M. K.: Northern hemisphere temperatures during the past millennium: Inferences, uncertainties, and limitations, Geophys. Res. Lett. , 26, 759-762, 1999.

Mann, M. E., Zhang, Z. H., Hughes, M. K., Bradley, R. S., Miller, S. K., Rutherford, S., and Ni, F. B.: Proxy-based reconstructions of hemispheric and global surface temperature variations over the past two millennia, Proc. Nat. Acad. Sci. U.S.A., 105, 13252-13257, doi:10.1073/pnas.0805721105, 2008.

Mann, M. E., Zhang, Z. H., Rutherford, S., Bradley, R. S., Hughes, M. K., Shindell, D., Ammann, C., Faluvegi, G., and Ni, F. B.: Global Signatures and Dynamical Origins of the Little Ice Age and Medieval Climate Anomaly, Science, 326, 1256-1260, doi:10.1126/science.1177303, 2009.

McGregor, S., Timmermann, A., and Timm, O.: A unified proxy for ENSO and PDO variability since 1650, Clim Past, 6, 1-17, doi:10.5194/cp-6-1-2010, 2010.

McShane, B. B., and Wyner, A. J.: A statistical analysis of multiple temperature proxies: Are reconstructions of surface temperatures over the last 1000 years reliable?, Annals of Applied Statistics, 5, 5-44, 2011.

Neukom, R., Luterbacher, J., Villalba, R., Kuttel, M., Frank, D., Jones, P. D., Grosjean, M., Wanner, H., Aravena, J. C., Black, D. E., Christie, D. A., D'Arrigo, R., Lara, A., Morales, M., Soliz-Gamboa, C., Srur, A., Urrutia, R., and von Gunten, L.: Multiproxy summer and winter surface air temperature field reconstructions for southern South America covering the past centuries, Clim. Dyn., 37, 35-51, doi:10.1007/s00382-010-0793-3, 2011.

Neukom, R., Nash, D. J., Endfield, G. H., Grab, S. W., Grove, C. A., Kelso, C., Vogel, C. H., and Zinke, J.: Multi-proxy summer and winter precipitation reconstruction for southern Africa over the last 200 years, Clim. Dyn., 42, 2713-2726, 2013.

Newman, M., Alexander, M. A., Ault, T. R., Cobb, K. M., Deser, C., Di Lorenzo, E., Mantua, N. J., Miller, A. J., Minobe, S., and Nakamura, H.: The Pacific decadal oscillation, revisited, J. Climate, 29, 4399-4427, 2016.

Nitta, T.: Convective activities in the tropical western Pacific and their impact on the Northern Hemisphere summer circulation, J. Meteor. Soc. Japan, 65, 373-390, 1987.

North, G. R., Bell, T. L., Cahalan, R. F., and Moeng, F. J.: Sampling errors in the estimation of empirical orthogonal functions, Monthly Weather Review, 110, 699-706, 1982.

PAGES2k-Consortium: A global multiproxy database for temperature reconstructions of the Common Era, Scientific Data, 2017.

PAGES-2k-Consortium: Continental-scale temperature variability during the past two millennia, Nat. Geosci. , 6, 339-346, doi:10.1038/ngeo1797

http://www.nature.com/ngeo/journal/vaop/ncurrent/abs/ngeo1797.html#supplementary-information, 2013.

Palmer, J. G., Cook, E. R., Turney, C. S., Allen, K., Fenwick, P., Cook, B. I., O'Donnell, A., Lough, J., Grierson, P., and Baker, P.: Drought variability in the eastern Australia and New Zealand summer drought atlas (ANZDA, CE 1500–2012) modulated by the Interdecadal Pacific Oscillation, Environ. Res. Lett. , 10, 124002, 2015.

Pei, L., Yan, Z., and Hui, Y.: Multidecadal variability of dry/wet patterns in eastern China and their relationship with the Pacific Decadal Oscillation in the last 413 years, Chin. Sci. Bull., 60, 97-108, doi:10.1360/n972014-00790, 2015.

Qian, C., and Zhou, T.: Multidecadal variability of North China aridity and its relationship to PDO during 1900–2010, J. Climate, 27, 1210-1222, doi:10.1175/JCLI-D-13-00235.1, 2014.

Qian, W., Hu, Q., Zhu, Y., and Lee, D.: Centennial-scale dry-wet variations in East Asia, Clim. Dyn., 21, 77-89, 2003a.

Qian, W. H., Chen, D., Zhu, Y., and Shen, H. Y.: Temporal and spatial variability of dryness/wetness in China during the last 530 years, Theor. Appl. Climatol. , 76, 13-29, doi:10.1007/s00704-003-0009-4, 2003b.

Ruan, C. Q., and Li, J. P.: An improvement in a time-scale decomposition statistical downscaling prediction model for summer rainfall over North China. Chinese Journal of Atmospheric Sciences, Chin. J. Atmos. Sci., 40, 215-226, 2016.

Schmidt, G. A., Kelley, M., Nazarenko, L., Ruedy, R., Russell, G. L., Aleinov, I., Bauer, M., Bauer, S. E., Bhat, M. K., and Bleck, R.: Configuration and assessment of the GISS ModelE2 contributions to the CMIP5 archive, Journal of Advances in Modeling Earth Systems, 6, 141-184, 2014.

Schneider, T.: Analysis of incomplete climate data: Estimation of mean values and covariance matrices and imputation of missing values, J. Climate, 14, 853-871, 2001.

Schubert, S. D., Stewart, R. E., Wang, H., Barlow, M., Berbery, E. H., Cai, W., Hoerling, M. P., Kanikicharla, K. K., Koster, R. D., and Lyon, B.: Global meteorological drought: A synthesis of current understanding with a focus on SST drivers of precipitation deficits, J. Climate, 29, 3989-4019, 2016.

Seftigen, K., Björklund, J., Cook, E., and Linderholm, H.: A tree-ring field reconstruction of Fennoscandian summer hydroclimate variability for the last millennium, Clim. Dyn., 44, 3141-3154, doi:10.1007/s00382-014-2191-8, 2015.

Shao, X., Huang, L., Liu, H., Liang, E., Fang, X., and Wang, L.: Reconstruction of precipitation variation from tree rings in recent 1000 years in Delingha, Qinghai, Science in China (Series D), 48, 939-949, 2005.

Shen, C., Wang, W. C., Gong, W., and Hao, Z.: A Pacific Decadal Oscillation record since 1470 AD reconstructed from proxy data of summer rainfall over eastern China, Geophys. Res. Lett. , 33, L03702, doi:10.1029/2005GL024804, 2006.

Shi, F., Yang, B., Charpentier Ljungqvist, F., and Fengmei, Y.: Multi-proxy reconstruction of Arctic summer temperatures over the past 1400 years, Clim. Res., 54, 113-128, doi:10.3354/cr01112, 2012.

Shi, F., Li, J., and Wilson, R. J. S.: A tree-ring reconstruction of the South Asian summer monsoon index over the past millennium, Scientific Reports, 4, doi:10.1038/srep06739, 2014.

Shi, F., Ge, Q., Yang, B., Li, J., Yang, F., Ljungqvist, F. C., Solomina, O., Nakatsuka, T., Wang, N., Zhao, S., Xu, C., Fang, K., Sano, M., Chu, G., Fan, Z., Narayan, P. G., and Muhammad, U. Z.: A multi-proxy reconstruction of spatial and temporal variations in Asian summer temperatures over the last millennium Clim. Change 131, 663-676, doi:10.1007/s10584-015-1413-3, 2015a.

Shi, F., Yang, B., Feng, J., Li, J., Yang, F., and Guo, Z.: Reconstruction of the Northern Hemisphere annual temperature change over the common era derived from tree rings Quat. Sci., 35, 1051-1063, doi:10.11928/j.issn.1001-7410.2015.05.01, 2015b.

Shi, F., Fang, K., Xu, C., Guo, Z., and Borgaonkar, H. P.: Interannual to centennial variability of the South Asian summer monsoon over the past millennium, Clim. Dyn., doi:10.1007/s00382-016-3493-9, 2016a.

Shi, Z., Xu, T., and Wang, H.: Sensitivity of Asian climate change to radiative forcing during the last millennium in a multi-model analysis, Glob. Planet. Chang., 139, 195-210, doi:http://dx.doi.org/10.1016/j.gloplacha.2016.02.007, 2016b.

Sigl, M., Winstrup, M., McConnell, J. R., Welten, K. C., Plunkett, G., Ludlow, F., Buntgen, U., Caffee, M., Chellman, N., Dahl-Jensen, D., Fischer, H., Kipfstuhl, S., Kostick, C., Maselli, O. J., Mekhaldi, F., Mulvaney, R., Muscheler, R., Pasteris, D. R., Pilcher, J. R., Salzer, M., Schupbach, S., Steffensen, J. P., Vinther, B. M., and Woodruff, T. E.: Timing and climate forcing of volcanic eruptions for the past 2,500 years, Nature, 523, 543-549, doi:10.1038/nature14565, 2015.

Song, F., and Zhou, T.: The crucial role of internal variability in modulating the decadal variation of the East Asian summer monsoon–ENSO relationship during the twentieth century, J. Climate, 28, 7093-7107, 2015.

Stuecker, M. F., Timmermann, A., Jin, F.-F., McGregor, S., and Ren, H.-L.: A combination mode of the annual cycle and the El Nino/Southern Oscillation, Nature Geosci, 6, 540-544, doi:10.1038/ngeo1826

http://www.nature.com/ngeo/journal/v6/n7/abs/ngeo1826.html#supplementary-information, 2013.

Tingley, M. P., and Huybers, P.: A Bayesian Algorithm for Reconstructing Climate Anomalies in Space and Time. Part I: Development and Applications to Paleoclimate Reconstruction Problems, J. Climate, 23, 2759-2781, doi:10.1175/2009jcli3015.1, 2010.

Wan, H., Zhang, X., Zwiers, F. W., and Shiogama, H.: Effect of data coverage on the estimation of mean and variability of precipitation at global and regional scales, J. Geophys. Res. [Atmos.], 118, 534-546, 2013.

Wang, B., Wu, R., and Fu, X.: Pacific–east Asian teleconnection: How does ENSO affect east Asian climate?, J. Climate, 13, 1517-1536, doi:10.1175/1520-0442(2000)013<1517:PEATHD>2.0.CO;2, 2000.

Wang, S., Gong, D., and Zhu, J.: Twentieth-century climatic warming in China in the context of the Holocene, Holocene, 11, 313-321, doi:10.1191/095968301673172698, 2001.

Wang, S., Cai, J., Mu, Q., Xie, Z., and Dong, W.: Climate change of annual precipitations in western China, Journal of Natural Resources, 17, 415-422, 2002.

Wang, S. W., and Zhao, Z. C.: An analyses of historical data of droughts and floods in last 500 years in China (in Chinese), Acta Geographica Sinica, 34, 329–341, 1979.

Wang, Y. M., Lean, J. L., and Sheeley, N. R.: Modeling the sun's magnetic field and irradiance since 1713, Astrophys. J., 625, 522-538, 2005.

Widmann, M., Goosse, H., van der Schrier, G., Schnur, R., and Barkmeijer, J.: Using data assimilation to study extratropical Northern Hemisphere climate over the last millennium, Clim Past, 6, 627-644, doi:10.5194/cp-6-627-2010, 2010.

Wu, B., Li, T., and Zhou, T.: Relative contributions of the Indian Ocean and local SST anomalies to the maintenance of the Western North Pacific anomalous anticyclone during the El Niño decaying summer*, J. Climate, 23, 2974-2986, 2010a.

Wu, R., and Wang, B.: A Contrast of the East Asian Summer Monsoon–ENSO Relationship between 1962–77 and 1978–93, J. Climate, 15, 3266-3279, doi:10.1175/1520-0442(2002)015<3266:ACOTEA>2.0.CO;2, 2002.

Wu, T., Yu, R., Zhang, F., Wang, Z., Dong, M., Wang, L., Jin, X., Chen, D., and Li, L.: The Beijing Climate Center atmospheric general circulation model: description and its performance for the present-day climate, Clim. Dyn., 34, 123-147, 2010b.

Wu, Z., and Huang, N.: Ensemble empirical mode decomposition: a noise assisted data analysis method, Adv. Adapt. Data Anal., 1, 1-41, doi:10.1142/S1793536909000047, 2009.

Wu, Z., Wang, B., Li, J., and Jin, F. F.: An empirical seasonal prediction model of the East Asian summer monsoon using ENSO and NAO, J. Geophys. Res. [Atmos.], 114, 2009.

Wu, Z., Li, J., Jiang, Z., and Ma, T.: Modulation of the Tibetan Plateau snow cover on the ENSO teleconnections: From the East Asian summer monsoon perspective, J. Climate, 25, 2481-2489, 2012.

Xie, S.-P., Hu, K., Hafner, J., Tokinaga, H., Du, Y., Huang, G., and Sampe, T.: Indian Ocean capacitor effect on Indo-western Pacific climate during the summer following El Niño, J. Climate, 22, 730-747, 2009.

Yang, B., Kang, S., Ljungqvist, F. C., He, M., Zhao, Y., and Qin, C.: Drought variability at the northern fringe of the Asian summer monsoon region over the past millennia, Clim. Dyn., 43, 845-859, 2014a.

Yang, B., Qin, C., Wang, J., He, M., Melvin, T. M., Osborn, T. J., and Briffa, K. R.: A 3,500-year tree-ring record of annual precipitation on the northeastern Tibetan Plateau, Proc. Nat. Acad. Sci. U.S.A., 111, 2903-2908, doi:10.1073/pnas.1319238111, 2014b.

Yang, F., Shi, F., Kang, S., Wang, S., Xiao, Z., Nakatsuka, T., and Shi, J.: Comparison of the dryness/wetness index in China with the Monsoon Asia Drought Atlas, Theor. Appl. Climatol. , 114, 553-566, doi:10.1007/s00704-013-0858-4, 2013a.

Yang, F., Wang, N., Shi, F., Ljungqvist, F. C., Wang, S., Fan, Z., and Lu, J.: Multi-proxy temperature reconstruction from the West Qinling Mountains, China, for the past 500 years, Plos One, 8, e57638, doi:10.1371/journal.pone.0057638, 2013b.

Yang, F., Wang, N., Shi, F., Ljungqvist, F. C., Zhao, S., and Liu, T.: The spatial distribution of precipitation over the West Qinling region, China, AD 1470–2000, Palaeogeogr. Palaeoclimatol. Palaeoecol., 443, 278-285, doi:10.1016/j.palaeo.2015.12.003, 2016.

Yu, R., and Zhou, T.: Seasonality and three-dimensional structure of interdecadal change in the East Asian monsoon, J. Climate, 20, 5344-5355, 2007.

Zhang, D.: Method to reconstruct climatic series for the past 500 years and its reliability, Collected Papers of Meteorological Science and Technology, 4, 17-26, 1983.

Zhang, D.: The method for reconstruction of the dryness/wetness series in China for the last 500 years and its reliability, in: The reconstruction of climate in China for historical times. Science Press, Beijing, China, 18-30, 1988.

Zhang, D.: Historical records of climate change in China, Quat. Sci. Rev., 10, 551-554, doi:http://dx.doi.org/10.1016/0277-3791(91)90049-Z, 1991.

Zhang, D., and Liu, C.: Continuation (1980-1992) of the yearly charts of dryness/wetness in China for the last 500 years period, Meteorological Monthly, 19, 41-45, 1993.

Zhang, D., Li, X., and Liang, Y.: Continuation (1992-2000) of the yearly charts of dryness/wetness in China for the last 500 years period, Journal of Applied Meteorological Science, 14, 379-384, 2003a.

Zhang, D.: A compendium of Chinese meteorological records of the last 3000 years, Nangjing: Jiangsu Education Publishing House, 2004.

Zhang, D.: Test of calibration on the paleoclimatic proxy data by using Chinese historical records, Advances in Climate Change Research, 6, 70-72, 2010.

Zhang, D. e., Wang, L., and Sun, X.: Reconstruction of grid precipitation anomaly in Eastern China from hitorical documents: New study on Chinese historical climate records, Quat. Sci., 23, 177-184, 2003b.

Zhang, L., and Zhou, T.: Drought over East Asia: A Review, J. Climate, 28, 3375-3399, doi:10.1175/JCLI-D-14-00259.1, 2015.

Zhang, Q., Cheng, G., Yao, T., Kang, X., and Huang, J.: A 2,326-year tree-ring record of climate variability on the northeastern Qinghai-Tibetan Plateau, Geophys. Res. Lett. , 30, 1739-1742, doi:10.1029/2003gl017425, 2003c.

Zhang, W., Jin, F.-F., Li, J., and Ren, H.-L.: Contrasting impacts of two-type El Niño over the western North Pacific during boreal autumn, Journal of the meteorological Society of Japan, 89, 563-569, 2011.

Zhang, W., Jin, F. F., Stuecker, M. F., Wittenberg, A. T., Timmermann, A., Ren, H. L., Kug, J. S., Cai, W., and Cane, M.: Unraveling El Niño's impact on the East Asian Monsoon and Yangtze River summer flooding, Geophys. Res. Lett. , 2016.

Zhao, S., Li, J., and Sun, C.: Decadal variability in the occurrence of wintertime haze in central eastern China tied to the Pacific Decadal Oscillation, Scientific Reports, 6, doi:10.1038/srep27424, 2016.

Zhao, Y., and Zhu, J.: Assessing quality of grid daily precipitation datasets in China in recent 50 years, Plateau Meteorology, 34, 50-58, 2015.

Zheng, F., Li, J., Li, Y., Zhao, S., and Deng, D.: Influence of the summer NAO on the spring-NAO-based predictability of the East Asian summer monsoon, J. Appl. Meteorol. Climatol., 2016.

Zheng, J., Wang, W., Ge, Q., Man, Z., and Zhang, P.: Precipitation variability and extreme events in eastern China during the past 1500 years, Terrestrial Atmospheric and Oceanic Sciences, 17, 579-592, 2006.

Zheng, J., Ge, Q., Hao, Z., Liu, H., Man, Z., Hou, Y., and Fang, X.: Paleoclimatology proxy recorded in historical documents and method for reconstruction on climate change, Quat. Sci., 34, 1186-1196, 2014a.

Zheng, J., Hao, Z., Fang, X., and Ge, Q.: Changing characteristics of extreme climate events during past 2000 years in China, Progress in Geography, 33, 3-12, 2014b.

Zhou, T., Gong, D., Li, J., and Li, B.: Detecting and understanding the multi-decadal variability of the East Asian summer monsoon recent progress and state of affairs, Meteorol. Z. , 18, 455-467, 2009.

Zhuo, Z., Gao, C., and Pan, Y.: Proxy evidence for China's monsoon precipitation response to volcanic aerosols over the past seven centuries, J. Geophys. Res. [Atmos.], 119, 6638-6652, doi:10.1002/2013JD021061, 2014.